Traversal-time wave-function analysis of resonance and nonresonance tunneling

D. Sokolovski, S. Brouard,* and J. N. L. Connor
Department of Chemistry, University of Manchester, Manchester M13 9PL, England
(Received 7 March 1994)

A generalized wave function is defined for an arbitrary real functional. Properties of the traversal-time wave function are investigated for one-dimensional scattering at a fixed energy. A Heisenberg-type uncertainty relation is derived from the traversal-time wave function. Traversal-time probability distributions for a Larmor clock measurement are studied in detail. The high-resolution limit of a traversal-time measurement is examined. The use of "fast" and "slow" arguments in a traversal-time analysis is discussed. The systems studied include free motion, resonance, and nonresonance tunneling through a double-δ-function potential, rectangular barrier, absorbing optical potential, and interaction with a slow oscillator.

PACS number(s): 03.65.Nk, 73.40.Gk

I. INTRODUCTION

It is often stated that one of the remaining unsolved problems in quantum mechanics is to determine the duration of a collision and, in particular, the time for a particle to tunnel through a potential barrier (for reviews, see Ref. [1]). Another commonly expressed view is that quantum mechanics in its standard form cannot describe these time parameters and therefore requires an extension or revision [2–4].

In conventional quantum mechanics, dynamical variables are represented by Hermitian operators and the wave function is interpreted as the probability amplitude for obtaining a particular value of the variable at a given time. However, for time parameters such as the tunneling time, it is not possible to define a wave function at a given instant of time because these parameters relate to a given duration of time. This is also true classically, where the classical traversal time is the time interval spent by a particle in a specified region of space.

An important approach to the quantum traversal-time problem exploits Feynman path-integral techniques [1,4–22]. Using this approach, we have shown [13–15] how the concept of a wave function can be generalized to a quantity which is represented classically by a functional that is nonlocal in time. In particular, the traversal-time wave function has been introduced in Ref. [13]. Having obtained this wave function, application to physical problems then follows well established lines [23].

The purpose of this paper is threefold. First, we investigate properties of the traversal-time wave function for one-dimensional scattering. The systems studied are free motion, resonance tunneling, rectangular barrier, absorbing optical potential, and interaction with a slow oscillator. Second, we discuss the measurement of the traversal time by a Larmor clock. Third, we show how a traversal-time analysis can be used to study the effect of external interactions on the tunneling.

This paper is arranged in the following way. Section II uses Feynman path-integral theory to derive a wave function for an arbitrary real functional defined along a classical path. Section III obtains the traversal-time wave function for a fixed collision energy and considers some of its general properties. The traversal-time wave function for free motion is analyzed in Sec. IV, where we show that it has some unusual properties. The traversal-time representation for resonance scattering is derived in Sec. V and we examine its behavior both on and off resonance. Section VI uses the results of Sec. IV to obtain the traversal-time wave function and transmission amplitude for a rectangular barrier potential, an absorbing potential, and an interaction with a slow oscillator. In Sec. VII we discuss an uncertainty relation for the traversal time and consider its measurement using a Larmor clock. The high-resolution limit of a traversal-time measurement is investigated in Sec. VIII. In Sec. IX we consider the use of "fast" and "slow" arguments in quantum mechanics. A traversal-time analysis for more general interactions is discussed in Sec. X. Our concluding remarks are in Sec. XI.

II. GENERALIZED WAVE FUNCTION FOR A QUANTITY REPRESENTED BY AN ARBITRARY REAL FUNCTIONAL

The probability (transition) amplitude $g(\Psi_2,t_2|\Psi_1,t_1)$ for a quantum particle prepared at time $t=t_1$ in an initial state Ψ_1, and then found in a final state Ψ_2 at the later time $t=t_2$, can be written as a sum over all Feynman paths [6]

$$g(\Psi_2,t_2|\Psi_1,t_1) = \int dx_2 \int Dx(\cdot) \int dx_1 \Psi_2^*(x_2) \times \exp\{iS[x(\cdot)]/\hbar\}\Psi_1(x_1) . \tag{2.1}$$

*Permanent address: Departamento de Física Fundamental y Experimental, Universidad de La Laguna, 38204 La Laguna, Tenerife, Spain.

In Eq. (2.1), $S[x(t)]$ is the classical action.

Consider an arbitrary real functional $F[x(t)]$, which represents some characteristic of the path $x(t)$. We can carry out the path integration in Eq. (2.1) in two steps. First, we sum the factor $\exp\{iS[x(\cdot)]/\hbar\}$ over only those paths along which $F[x(t)]$ takes a given value f, i.e., $F[x(t)]=f$. We can write

$$\eta(f)=\int dx_2 \int Dx(\cdot) \int dx_1 \Psi_2^*(x_2)\delta(F[x(\cdot)]-f) \times \exp\{iS[x(\cdot)]/\hbar\}\Psi_1(x_1) , \tag{2.2}$$

where $\delta(x)$ is the Dirac δ function. In the same way that a conventional wave function in the coordinate representation $\Psi(x,t)$ gives the amplitude for the coordinate to equal x at time t, the function $\eta(f)$ is the amplitude to have the value f in the transition $(\Psi_1,t_1)\rightarrow(\Psi_2,t_2)$. For this reason, we will call $\eta(f)$ the (generalized) wave function in the f representation. It differs by a normalization factor from the amplitude distribution $\sigma_A(a)$ introduced in Ref. [13]. Note that $\eta(f)$ must vanish identically for those values of f which the functional F cannot take.

In the second step, we integrate Eq. (2.2) over all possible values of f (assumed to be $-\infty<f<\infty$), which yields

$$g(\Psi_2,t_2|\Psi_1,t_1)=\int_{-\infty}^{\infty}\eta(f)df . \tag{2.3}$$

Thus if the wave function $\eta(f)$ is known, $g(\Psi_2,t_2|\Psi_1,t_1)$ can be evaluated as a simple one-dimensional quadrature.

We can derive an alternative expression for $\eta(f)$ by replacing the δ function in Eq. (2.2) by its usual integral representation [13]. We then obtain

$$\eta(f)=\frac{1}{2\pi\hbar}\int_{-\infty}^{+\infty}d\lambda \exp(i\lambda f/\hbar)g(\lambda) , \tag{2.4}$$

where

$$g(\lambda)\equiv\int dx_2\int Dx(\cdot)\int dx_1\Psi_2^*(x_2) \times\exp\{iS_\lambda[x(\cdot)]/\hbar\}\Psi_1(x_1) \tag{2.5}$$

is the transition amplitude between the same initial and final states, but governed by a new action $S_\lambda[x(t)]\equiv S[x(t)]-\lambda F[x(t)]$.

Equation (2.4) is a generalization of the familiar relation between the momentum and coordinate representations [23], with f playing the role of the coordinate and λ the momentum. Indeed, the exponential factor in Eq. (2.4) is an eigenfunction of the operator $-i\hbar(\partial/\partial f)$, which represents the variable "conjugate" to f. Equation (2.4) shows that to calculate $\eta(f)$, one needs to know $g(\lambda)$, for all values of λ. Note also that $\eta(f)$ is normalized by Eq. (2.3) rather than the condition $\int_{-\infty}^{\infty}|\eta(f)|^2df=1$.

III. TRAVERSAL TIME REPRESENTATION FOR TIME-INDEPENDENT SCATTERING

We now consider the question of how much time (duration) a one-dimensional particle of mass m and wave number k spends in a region $[a,b]$. Classically, this duration is given by the traversal-time functional

$$t_{ab}^{\rm cl}[x(t)]\equiv\int_{t_1}^{t_2}\theta_{ab}(x(t))dt ,$$

where $\theta_{xz}(y)=1$ if $x\le y\le z$ and 0 otherwise, and $x(t)$ is the particle's trajectory [7–10]. Quantally, all information about the probable values of a physical quantity, e.g., the position of an electron in a hydrogen atom, is contained in the wave function. Therefore, for the present problem we must first obtain the wave function in the traversal-time representation, i.e., $\eta(\tau)$.

A. Traversal-time wave function

We obtain the traversal-time wave function by the method of Sec. II. One-dimensional elastic scattering by a potential $V(x)$ is described by reflection and transmission amplitudes $R(k)$ and $T(k)$, which are the probability amplitudes for a particle with initial momentum $\hbar k$ at $t_1\rightarrow-\infty$ to have momenta $-\hbar k$ and $\hbar k$ after the collision at $t_2\rightarrow+\infty$, respectively. A simple method to calculate $\eta(\tau)$ for the transmitted particle is to apply Eq. (2.5) to a wave packet whose initial spread of energies tends to zero, as described in Ref. [13]. It is then readily seen that the action $S_\lambda[x(t)]\equiv S[x(t)]-\lambda t_{ab}^{\rm cl}[x(t)]$ in Eq. (2.5) corresponds to that for a particle interacting with $V(x)$ plus an additional potential $\lambda\theta_{ab}(x)$. Replacing λ by W and denoting the transmission amplitude for the *composite potential* $V(x)+W\theta_{ab}(x)$ by $T(k,W)$, we have [13] (see also Ref. [18])

$$\eta_{ab}^T(k,\tau)=\frac{1}{2\pi\hbar}\int_{-\infty}^{+\infty}dW\exp(iW\tau/\hbar)T(k,W) \tag{3.1}$$

In Eq. (3.1), $\eta_{ab}^T(k,\tau)$ is the amplitude to have momentum $\hbar k$ before and after the collision and, in addition, to spend inside $[a,b]$ a duration τ. Note that for any path, $t_{ab}^{\rm cl}[x(t)]$ can only have a non-negative value, which does not exceed the total duration of motion t_2-t_1. Furthermore, since the collision begins in the distant past where $t_1\rightarrow-\infty$ and is completed in the distant future where $t_2\rightarrow\infty$, we have $\eta_{ab}^T(k,\tau)\equiv0$ for $\tau<0$, but $\eta_{ab}^T(k,\tau)$ can be nonzero for any $\tau\ge0$.

For the reflected particle, $T(k,W)$ in Eq. (3.1) must be replaced by $R(k,W)$, the reflection amplitude for the composite potential. In problems with more than two channels, the appropriate S-matrix element for the composite potential must be used.

Finally, inverting the Fourier transform (3.1), or using Eq. (2.3), we obtain the traversal time representation for $T(k)$

$$T(k)=\int_0^{\infty}\eta_{ab}^T(k,\tau)d\tau . \tag{3.2}$$

This result will often be used in the following sections.

B. General properties of the traversal-time wave function

The following general quantum-mechanical rules apply to the traversal-time wave function, where we will suppress the indices defining the scattering channel, the region $[a,b]$, and the wave number and simply write $\eta(\tau)$

from now on.

(i) If no measurements are made, the duration spent by the particle in $[a,b]$ cannot be determined, in accordance with the uncertainty principle. This point is discussed further in Ref. [14].

(ii) If we measure the quantum traversal time by a device, the probability amplitude that the result of the measurement be $\mathcal{T}$ is given by (cf. Ref. [6], pp. 106–108)

$$\Psi(\mathcal{T})=\int_0^\infty G(\mathcal{T},\tau)\eta(\tau)d\tau\ , \tag{3.3}$$

where $G(\mathcal{T},\tau)$ is a function peaked around $\tau=\mathcal{T}$ whose width determines the accuracy (resolution) of the measurement. Equivalently, to measure the value of the traversal time with a given accuracy, we must project $\eta(\tau)$ onto a state $G(\mathcal{T},\tau)$ sufficiently localized on the τ coordinate. The probability to have the result $\mathcal{T}$, denoted $P(\mathcal{T})$, is then given by $P(\mathcal{T})=|\Psi(\mathcal{T})|^2$. In the limiting case of an infinitely accurate measurement $G(\mathcal{T},\tau)\to\delta(\tau-\mathcal{T})$ and for a smooth $\eta(\tau)$, the expectation value of the traversal time $\langle\tau\rangle$ is given by

$$\langle\tau\rangle=\int_0^\infty \tau|\eta(\tau)|^2d\tau\Big/\int_0^\infty|\eta(\tau)|^2d\tau\ . \tag{3.4}$$

Equation (3.4) is analogous to the standard expression for $\langle x\rangle$, the expectation value for the position of the particle.

(iii) The transition amplitude $g_1(\Psi_2,t_2|\Psi_1,t_1)$ for a particle governed by an action $S_1[x(t)]$ can be written in terms of $\eta(\tau)$, calculated for an action $S[x(t)]$, as

$$g_1(\Psi_2,t_2|\Psi_1,t_1)=\int_0^\infty A(\tau)\eta(\tau)d\tau\ , \tag{3.5}$$

where $A(\tau)=\eta_1(\tau)/\eta(\tau)$ and $\eta_1(\tau)$ is the amplitude (2.2) for the action $S_1[x(t)]$. Equation (3.5) is simply an identity.

(iv) For the specific case $S_1[x(t)]=S[x(t)]+f(t_{ab}^{\rm cl}[x(t)])$, where f is an arbitrary function, we have

$$\eta_1(\tau)=\exp[if(\tau)/\hbar]\eta(\tau) \tag{3.6}$$

because the δ function in Eq. (2.2) makes $S_1[x(t)]-S[x(t)]$ have the same value $f(\tau)$ for all paths that spend in $[a,b]$ a duration τ. Provided $\eta(\tau)$ is known, we have the important, yet simple, result

$$g_1(\Psi_2,t_2|\Psi_1,t_1)=\int_0^\infty\exp[if(\tau)/\hbar]\eta(\tau)d\tau\ . \tag{3.7}$$

The statements (i)–(iv) are also valid for an arbitrary real functional $F[x(t)]$ provided the integration limits in Eqs. (3.3)–(3.5) and (3.7) are changed to the values actually taken by the functional.

In the following three sections, we will explore the properties of the wave function $\eta_{ab}^T(k,\tau)$ for the cases of free motion, resonance tunneling, rectangular barrier, absorbing potential, and an interaction with a slow oscillator.

IV. TRAVERSAL-TIME WAVE FUNCTION FOR FREE MOTION

In this section we obtain a series representation for the wave function $\eta_0(k,\tau)$ for the important case of a particle moving in free space, $V(x)=0$, and discuss its properties. According to Eq. (3.1), $\eta_0(k,\tau)$ is the Fourier transform of the transmission amplitude $T_0(k,W)$ for the rectangular potential $W\theta_{ab}(x)$, with W ranging from $-\infty$ to $+\infty$.

Instead of k and W, it is convenient to introduce the dimensionless variables

$$\beta\equiv k(b-a)$$

and

$$z\equiv[2m(W-E)]^{1/2}(b-a)/\hbar\ ,$$

respectively, where E is the collision energy. In terms of β and z, the transmission amplitude can be written as [24]

$$T_0(\beta,z)=\frac{-4i\beta z\exp(-i\beta)}{(z-i\beta)^2\exp(z)-(z+i\beta)^2\exp(-z)}\ . \tag{4.1}$$

By analytic continuation, Eq. (4.1) is valid in the entire complex W plane.

A. Series representation for $\eta_0(k,\tau)$

We have not been able to evaluate the Fourier transform

$$\eta_0(k,\tau)=\frac{1}{2\pi\hbar}\int_{-\infty}^{+\infty}dW\exp(iW\tau/\hbar)T_0(k,W) \tag{4.2}$$

analytically. However, it is possible to obtain a series representation for $\eta_0(k,\tau)$ using the method of residues, as we now explain.

For $\beta=0$, $T_0(\beta,z)$ has an infinite number of poles lying along the Imz axis at $z_n=(n-1)\pi i$, with $n=1,2,\ldots$. For $\beta=\infty$, the poles lie at $z_n=n\pi i$. For finite values of β, the pole positions are obtained from

$$\exp(z_n)=(-1)^{n-1}\frac{z_n+i\beta}{z_n-i\beta},\quad n=1,2,\ldots\ . \tag{4.3}$$

As β increases from 0 to ∞, each pole trajectory traces out a loop in the first quadrant of the complex z plane, as illustrated in Fig. 1 for $n\le 6$. In the complex W plane, the pole positions are given by

$$W_n=\hbar^2z_n^2/[2m(b-a)^2]+E,\quad n=1,2,\ldots\ . \tag{4.4}$$

The residues of $T_0(\beta,z)$ are

$$\mathrm{Res}_n\,T_0(\beta,z)=-2i\beta\exp(-i\beta)(-1)^{n-1}\frac{z_n}{z_n^2+\beta^2+2i\beta}\ ,\quad n=1,2,\ldots\ . \tag{4.5}$$

Next we return to the integral (4.2), change variables from W to z, and close the integration contour in the first quadrant of the complex z plane so that Cauchy's theorem can be applied. The result can be written

$$\eta_0(k,\tau)=\sum_{n=1}^{\infty}(-1)^{n-1}a_n\exp(iW_n\tau/\hbar)\ . \tag{4.6}$$

Using Eqs. (4.4) and (4.5), we find that the coefficients $\{a_n\}$ are given by

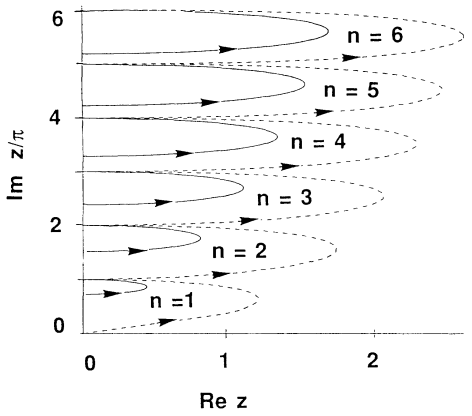

FIG. 1. Pole trajectories $n=0$–6 of $T(\beta,z)$ in the complex z plane, where $z\equiv[2m(W-E)]^{1/2}(b-a)/\hbar$, as $\beta\equiv k(b-a)$ increases from 0 to ∞. The arrows indicate the direction of increasing β (a) free motion (dashed line) and (b) double-δ-function potential with $\chi=5$ (solid line).

$$a_n=\frac{2\exp(-i\beta)}{\tau_0}\frac{z_n^2}{z_n^2+\beta^2+2i\beta}$$
$$=\frac{2\exp(-i\beta)}{\tau_0}\frac{(W_n-E)}{(W_n+i\hbar/\tau_0)},\quad n=1,2,\ldots, \tag{4.7}$$

where

$$\tau_0=m(b-a)/(\hbar k)$$

is the time it takes a classical particle with momentum $\hbar k$ to traverse $[a,b]$.

B. Properties of $\eta_0(k,\tau)$

We next use the series representation (4.6) to investigate some properties of $\eta_0(k,\tau)$.

(i) A perturbative solution of the pole formula (4.3) shows that for large n

$$z_n^2=-(n-1)^2\pi^2+4i\beta+O(1/n^2)\ .$$

Hence, for $n\to\infty$, Eq. (4.4) yields

$$W_n=-(n-1)^2\frac{\pi^2\hbar^2}{2m(b-a)^2}+E+\frac{2i\hbar}{\tau_0}+O\left[\frac{1}{n^2}\right] \tag{4.8}$$

and Eq. (4.7) becomes

$$\lim_{n\to\infty} a_n=2\exp(-i\beta)/\tau_0\ . \tag{4.9}$$

Equations (4.8) and (4.9) demonstrate that the nth term in the series representation (4.6) for $\eta_0(k,\tau)$ does not tend to zero. In fact, the series (4.6) is oscillatory and must be interpreted as a distribution. Its behavior is that of a Jacobi theta function of the fourth kind, $\theta_4(\nu|z)$, on its boundary $z=x$ [25]. To see this, note that the tail of the series can be written

$$S=\frac{2}{\tau_0}\exp(iE\tau/\hbar-2\tau/\tau_0-i\beta)$$
$$\times\sum_{l=1}^{\infty}(-1)^l\exp\left[-i\frac{\pi^2l^2\hbar\tau}{2m(b-a)^2}\right]\ .$$

Now, by definition, for $\mathrm{Im}\,z>0$ [25]

$$\theta_4(\nu|z)\equiv1+2\sum_{l=1}^{\infty}(-1)^l\exp(i\pi l^2z)\cos(2\pi l\nu)\ ,$$

so that S can be expressed as

$$S=\frac{1}{\tau_0}\exp(iE\tau/\hbar-2\tau/\tau_0-i\beta)$$
$$\times\left[\theta_4\left[0\left|-\frac{\pi\hbar\tau}{2m(b-a)^2}\right.\right]-1\right]\ .$$

Oscillatory θ-function expansions similar to Eq. (4.6) have also been found in several other physical problems [26]. Note that in practice the series (4.6) can be truncated at a large value of n when calculating physical quantities, such as $\Psi(\mathcal{T})$ in Eq. (3.3). This is because the resulting integrals will rapidly tend to zero as $n\to\infty$, since they possess highly oscillating integrands.

(ii) The integral $\int_0^\infty|\eta_0(k,\tau)|^2d\tau$ is divergent. To show this we formally use Parseval's theorem (Ref. [25], p. 139, item 4.11-11) to write

$$\int_0^\infty|\eta_0(k,\tau)|^2d\tau=\frac{1}{2\pi\hbar}\int_{-\infty}^{\infty}|T_0(k,W)|^2dW\ . \tag{4.10}$$

Now consider the range $W<E$, so that z is pure imaginary. Equation (4.1) gives

$$|T_0(k,W)|^2=|T_0(\beta,|z|)|^2$$
$$=\frac{4\beta^2|z|^2}{4\beta^2|z|^2+(\beta^2-|z|^2)^2\sin^2(|z|)}\ . \tag{4.11}$$

Next replace Eq. (4.11) by the smaller quantity $4\beta^2|z|^2/[4\beta^2|z|^2+(\beta^2-|z|^2)^2]$ and insert it into Eq. (4.10). We then find that the integral diverges logarithmically for $W\to-\infty$, which proves our original statement. An application of property (ii) will be discussed in Sec. VIII.

(iii) The contribution of each pole to the residue sum (4.6) decays exponentially with τ because all the pole positions $\{W_n\}$ lie in the upper half of the complex W plane. We have verified numerically that for a fixed E, the $n=1$ pole has the smallest imaginary part. The largest time scale associated with $\eta_0(k,\tau)$ is therefore approximately $\tau_{\max}=\hbar/\mathrm{Im}W_1$. Note that $\tau_{\max}$ can be interpreted as the "effective size" of $\eta_0(k,\tau)$ along the τ coordinate, just like the Bohr radius a_0 for the ground-state radial wave function $\exp(-r/a_0)$ of a hydrogen atom determines the effective size of the atom. We will show below that $\tau_{\max}$ tends to infinity in the classical limit $\beta\to\infty$.

(iv) If we compare the de Broglie wavelength of the incident particle $2\pi/k$ to the width of the region $b-a$, we find that there are three different cases.

(a) (Ultra)quantum case ($\beta\ll1$). For small β, the pole formula (4.3) has the perturbative solutions

$$z_1^2 = 2i\beta + O(\beta^2)$$

and

$$z_n^2 = -(n-1)^2\pi^2 + 4i\beta + O(\beta^2), \quad n = 2,3,\ldots$$

so that the series for $\eta_0(k,\tau)$ can be written in the form

$$\eta_0(k,\tau) \approx \frac{1}{\tau_0}\exp(-\tau/\tau_0) + \frac{2}{\tau_0}\sum_{n=2}^{\infty}(-1)^{n-1}\exp\left[-i\frac{\pi^2(n-1)^2}{2\beta}\frac{\tau}{\tau_0}\right] \times \exp(-2\tau/\tau_0) . \quad (4.12)$$

Equation (4.12) shows that the leading $n=1$ pole contributes an exponential term with a lifetime $\tau_{\max}=\tau_0$. The terms in the sum with $n>1$ are exponentials with an envelope $\exp(-2\tau/\tau_0)$, which oscillate with high angular frequencies $\pi^2(n-1)^2/(2\beta\tau_0)$ for $n=2,3,\ldots$. Thus in the limit $\beta\to 0$ we can simply approximate $\eta_0(k,\tau)$ by $\tau_0^{-1}\exp(-\tau/\tau_0)$. Note that neglect of the highly oscillatory terms with $n>1$ is only justified if we are not interested in the detailed behavior of $\eta_0(k,\tau)$ on a τ scale finer than approximately equal to $4\tau_0\beta/\pi$.

Figure 2(a) shows the convoluted wave function

$$\bar{\eta}_0(k,\tau) \equiv \frac{1}{\pi^{1/2}\gamma\tau_0}\int_0^{\infty}\exp\left[-\frac{(\tau-\tau')^2}{\gamma^2\tau_0^2}\right]\eta_0(k,\tau')d\tau'$$

plotted versus the reduced time $T=\tau/\tau_0$ for $\beta=0.001$ and $\gamma=0.015$ obtained by term-by-term integration of Eq. (4.6). The smooth exponential decay of $\bar{\eta}_0(k,\tau)$ is clearly visible.

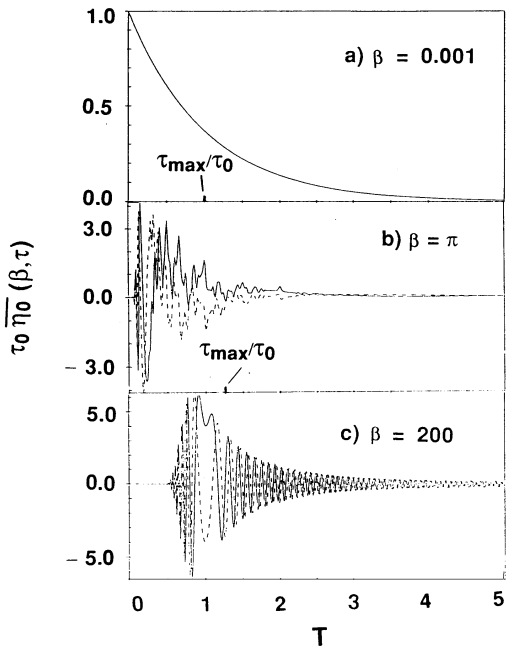

FIG. 2. Real part (solid line) and imaginary part (dashed line) of $\tau_0\bar{\eta}_0(\beta,\tau)$ with $\gamma=0.015$ versus the reduced time $T=\tau/\tau_0$ for (a) $\beta=0.001$. The imaginary part is too small to be visible on the scale of the drawing in this case. (b) $\beta=\pi$; (c) $\beta=200$. The corresponding values of $\tau_{\max}/\tau_0$ are (a) 1.0, (b) 1.26, and (c) 2026.66, respectively.

(b) Intermediate case ($\beta\approx 1$). When the de Broglie wavelength is comparable to $b-a$, the pole positions for $n\lesssim\beta$ must be determined numerically from Eq. (4.3), which also allows $\tau_{\max}=\hbar/\mathrm{Im}W_1$ to be calculated. The contribution from poles with $n\gg\beta$ is essentially the same as in case (a) and $\eta_0(k,\tau)$ can be computed by truncating the series (4.6) at a sufficiently large value of n.

Figure 2(b) shows $\bar{\eta}_0(k,\tau)$ versus T for $\beta=\pi$ and $\gamma=0.015$. The convoluted wave function has a complicated shape which tends to zero for $\tau>\tau_{\max}$.

(c) Semiclassical case ($\beta\gg 1$). A perturbative solution of the pole formula (4.3) for $|\beta/z_n|\gg 1$ results in

$$z_n \approx n\pi i + 2n\pi/\beta, \quad n=1,2,\ldots$$

and using Eq. (4.4) gives

$$W_n \approx E - \frac{(\hbar\pi n)^2}{2m(b-a)^2} + i\frac{2(\hbar\pi n)^2}{\beta m(b-a)^2}, \quad n=1,2,\ldots \quad (4.13)$$

so that $\mathrm{Im}W_n = 2n^2\pi^2\hbar/(\beta^2\tau_0)$ and $\tau_{\max}=\hbar/\mathrm{Im}W_1 = \beta^2\tau_0/2\pi^2$. Since $\tau_{\max}\gg\tau_0$ in this case, $\eta_0(k,\tau)$ tends to zero rather slowly for large values of τ. This can come as a surprise, because one expects $\eta_0(k,\tau)$ to be sharply peaked around the classical value τ_0 and to tend to $\delta(\tau-\tau_0)$ as $\hbar\to 0$.

Figure 2(c) shows $\bar{\eta}_0(k,\tau)$ versus T for $\beta=200$ and $\gamma=0.015$ obtained by summing (4.6) for $n\gg\beta/\pi$. Evidently, $\eta_0(k,\tau)$ is highly oscillatory except for a small vicinity $\Delta\tau$ of $\tau=\tau_0$. In this vicinity $\mathrm{Re}\eta_0(k,\tau)$ remains positive while $\mathrm{Im}\eta_0(k,\tau)$ changes sign so that Eq. (3.2) for $T(k)$ tends to 1 for $\mathrm{Re}\eta_0(k,\tau)$ and to 0 for $\mathrm{Im}\eta_0(k,\tau)$.

The width $\Delta\tau$ can be evaluated by noting from Eq. (4.2) that $\eta_0(k,\tau)=\delta(\tau-\tau_0)$ requires $T(k,W)=\exp(-iW\tau_0/\hbar)$. Now for $z\approx i\beta$ with $\beta\gg 1$, we can write Eq. (4.1) in the form

$$T(k,W) \approx \exp(z-i\beta) = \exp\{-i[W\tau_0/\hbar + W^2\tau_0^2/(2\hbar^2\beta) + O(W^3/E^{5/2})]\} .$$

The range of W for which the second term in the exponent can be neglected is $\Delta W \approx 2(2\beta)^{1/2}\hbar/\tau_0$ and therefore $\Delta\tau=\hbar/\Delta W \approx \tau_0/[2(2\beta)^{1/2}] \ll \tau_{\max}$.

An improved approximation for $\eta_0(k,\tau)$ can be obtained for $z\approx i\beta$ with $\beta\gg 1$ by first writing

$$T_0(\beta,z) \approx \frac{4i\beta z}{(z+i\beta)^2}\exp(z-i\beta) .$$

A stationary-phase evaluation of Eq. (4.2) then yields

$$\eta_0(k,\tau) \approx \frac{4\tau_0}{(\tau+\tau_0)^2}\left[\frac{\tau_0}{\tau}\right]^{1/2}\left[\frac{\beta}{2\pi}\right]^{1/2} \times \exp\left[i\frac{\beta(\tau-\tau_0)^2}{2\tau\tau_0} - i\frac{\pi}{4}\right] . \quad (4.14)$$

For $|\tau-\tau_0| \ll \tau_0/\beta^{1/3}$, Eq. (4.14) reduces to the simpler approximation

$$\eta_0(k,\tau)\approx\frac{1}{\tau_0}\left[\frac{\beta}{2\pi}\right]^{1/2}\exp\left[i\frac{\beta(\tau-\tau_0)^2}{2\tau_0^2}-i\frac{\pi}{4}\right],$$

a result we obtained in Ref. [15]. Note that $\eta_0(k,\tau)\to\delta(\tau-\tau_0)$ for $\beta\to\infty$.

V. TRAVERSAL-TIME WAVE FUNCTION FOR RESONANCE TUNNELING

Resonance transmission through a double-barrier potential is often associated with a long time delay as the tunneling particle becomes "trapped" in the well between the two barriers. In this section we investigate $\eta(k,\tau)$ both on and off resonance to see if it possesses properties characteristic of resonance tunneling.

A. Double-δ-function potential barrier

The simplest model that exhibits resonance tunneling consists of two δ-function barriers, located at $x=a$ and b, respectively:

$$2mV(x)/\hbar^2=2\Omega[\delta(x-a)+\delta(x-b)]\ . \tag{5.1}$$

The transmission amplitude for this potential can be written in the form [27]

$$T_{\delta\delta}(k)=\frac{4\beta^2\exp(-i\beta)}{\chi^2\exp(i\beta)-(2i\beta-\chi)^2\exp(-i\beta)}\ , \tag{5.2}$$

where

$$\chi=2\Omega(b-a)\ .$$

For large Ω, the barriers are almost impenetrable and the potential (5.1) supports quasistationary states with resonance energies $\{E_n\}$ and halfwidths $\{\Gamma_n/2\}$ determined by the positions of the poles of $T_{\delta\delta}(k)$ in the complex energy plane. With the help of Eq. (5.2), we find that the resonance energies are given approximately by the quantization rule for a particle in a box of length $b-a$

$$E_n=\frac{\pi^2\hbar^2n^2}{2m(b-a)^2}+O\left[\frac{1}{\chi}\right],\quad n=1,2,\ldots \tag{5.3}$$

and that the resonance widths are

$$\frac{\Gamma_n}{2}=\frac{2\hbar^2(\pi n)^3}{m\chi^2(b-a)^2}+O\left[\frac{1}{\chi^3}\right],\quad n=1,2,\ldots . \tag{5.4}$$

As a result, when the incident energy coincides with one of the quasistationary states, we have $T_{\delta\delta}(k)=-1$, which leads to complete transparency of the double barrier (5.1).

B. Series representation for $\eta_{\delta\delta}(k,\tau)$

We obtain the traversal-time wave function $\eta_{\delta\delta}(k,\tau)$ for the well region $[a,b]$ by inserting in Eq. (3.1) the transmission amplitude $T_{\delta\delta}(k,W)$ for the composite potential $V(x)+W\theta_{ab}(x)$. Using standard techniques, we find that $T_{\delta\delta}(k,W)$ is a generalization of Eqs. (4.1) and (5.2), namely,

$$T_{\delta\delta}(\beta,z)=\frac{-4i\beta z\exp(-i\beta)}{[z-i(\beta+i\chi)]^2\exp(z)-[z+i(\beta+i\chi)]^2\exp(-z)}\ . \tag{5.5}$$

We again use the method of residues to obtain a series representation for $\eta_{\delta\delta}(k,\tau)$. The positions of the poles $\{z_n\}$ of $T_{\delta\delta}(\beta,z)$ in the complex z plane are given by Eq. (4.3), except that $i\beta$ is replaced by $i(\beta+i\chi)$. The pole positions trace out loops in the complex z plane as β increases from 0 to ∞, as illustrated in Fig. 1 for $n\le 6$. For $\chi\gg\beta$ and $\chi\gg N\pi$, the positions of the lowest poles in the complex W plane are

$$W_n=E-E_n+O\left[\frac{1}{\chi}\right]+i\left[\frac{\Gamma_n}{2}\left[\frac{E}{E_n}\right]^{1/2}+O\left[\frac{1}{\chi^3}\right]\right],\quad n=1,2,\ldots,N\ . \tag{5.6}$$

The residues of $T_{\delta\delta}(\beta,z)$ are given by Eq. (4.5) provided $\beta^2+2i\beta$ is replaced by $(\beta+i\chi)^2+2i(\beta+i\chi)$. In the limits $\chi\gg\beta$ and $\chi\gg N\pi$, we have

$$\lim_{\chi\to\infty}\eta_{\delta\delta}(k,\tau)=\exp(-i\beta)\sum_{n=1}^{N}(-1)^{n-1}\frac{\Gamma_n}{2\hbar}\left[\frac{E}{E_n}\right]^{1/2}\exp\left\{i\left[E-E_n+i\frac{\Gamma_n}{2}\left[\frac{E}{E_n}\right]^{1/2}\right]\frac{\tau}{\hbar}\right\}+Q\ , \tag{5.7}$$

where Q includes contributions from those poles for which Eq. (5.6) no longer holds.

C. Properties of $\eta_{\delta\delta}(k,\tau)$

We can use Eq. (5.7) to study the on- and off-resonance behavior of $\eta_{\delta\delta}(k,\tau)$ in the limits $\chi\gg\beta$ and $\chi\gg N\pi$. For $E\neq E_j$, with $j=1,2,\ldots,N$, all terms in Eq. (5.7) oscillate rapidly so that the transmission amplitude [From Eq. (3.2)]

$$T_{\delta\delta}(k)=\int_0^\infty\eta_{\delta\delta}(k,\tau)d\tau \tag{5.8}$$

will be small.

On the other hand, at a resonance $E=E_j$, the jth term in the sum (5.7) has the form

$$-(\tfrac{1}{2}\Gamma_j/\hbar)\exp(-\tfrac{1}{2}\Gamma_j\tau/\hbar)$$

since $\beta\approx j\pi$ from Eq. (5.3). This term is nonoscillatory and decays with a lifetime $\hbar/\frac{1}{2}\Gamma_j$. It is responsible for the complete transparency of the double-barrier potential since the right-hand side of Eq. (5.8) yields -1 in this case.

More generally for $E\approx E_j$, the jth term in Eq. (5.7) can

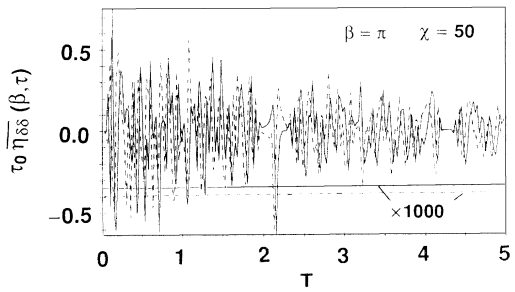

FIG. 3. Real part (solid line) and imaginary part (dashed line) of $\tau_0\bar{\eta}_{\delta\delta}(\beta,\tau)$ with $\gamma=0.015$, $\beta=\pi$, and $\chi=50$ vs the reduced time $T=\tau/\tau_0$. The nearly horizontal solid line is the first term ($\times 1000$) in the residue series for $\tau_0\bar{\eta}_{\delta\delta}(\beta,\tau)$, while the nearly horizontal dashed line is $-\tau_0(\frac{1}{2}\Gamma_1/\hbar)\exp(-\frac{1}{2}\Gamma_1\tau/\hbar)$ ($\times 1000$), where $\frac{1}{2}\Gamma_1$ is calculated using the first term of Eq. (5.4).

be approximated by

$$-(\tfrac{1}{2}\Gamma_j/\hbar)\exp[i(E-E_j+i\tfrac{1}{2}\Gamma_j)\tau/\hbar] .$$

Equation (5.8) then yields the Breit-Wigner approximation for the transmission amplitude

$$T_{\delta\delta}^{(\mathrm{BW})}(E)\approx\frac{-i\frac{1}{2}\Gamma_j}{E-E_j+i\frac{1}{2}\Gamma_j} . \tag{5.9}$$

For $E\approx E_j$, terms in the sum (5.7) with $n\neq j$ remain oscillatory. In particular, the $(j+1)$th term has a period of oscillation of $2\pi\hbar/(E_{j+1}-E_j)$. With the help of Eq. (5.3) this period is readily seen to be approximately $2\tau_0$, which is short compared to the long lifetime of the resonance $\hbar/\frac{1}{2}\Gamma_j$ [see Eq. (5.4)]. When $E\approx E_j$, the contribution of the $(j+1)$th term to $T_{\delta\delta}(k)$ is approximately

$$-i\tfrac{1}{2}\Gamma_{j+1}(E_j/E_{j+1})^{1/2}/(E_{j+1}-E_j) ,$$

which is small compared to the Breit-Wigner contribution (5.9). However, terms with $n\neq j$ for $E\approx E_j$ cannot be neglected if more detailed information on $\eta_{\delta\delta}(k,\tau)$ is required.

In summary, for the case of resonance tunneling we have found, as expected, that the traversal-time wave function tends to zero much slower than in the free-particle case. Its on-resonance behavior is characterized by the formation of a slowly decaying nonoscillatory tail in the series representation (5.7), which is responsible for the absolute transparency of a symmetric double barrier. Figure 3 shows the convoluted wave function $\bar{\eta}_{\delta\delta}(k,\tau)$ for $\beta=\pi$, $\chi=50$, and $\gamma=0.015$. Note that the long tail $-(\frac{1}{2}\Gamma_1/\hbar)\exp(-\frac{1}{2}\Gamma_1\tau/\hbar)$, is lost in the background oscillatory contributions from poles with $n>1$ in this case.

VI. TRAVERSAL-TIME WAVE FUNCTION FOR ADDITIONAL INTERACTIONS

Equation (3.6) provides a simple way to calculate the traversal-time wave function for an additional interaction of the form $f(t_{ab}^{\mathrm{cl}}[x(t)])$, provided we know the wave function for the unperturbed problem. The corresponding transmission amplitude can then be obtained from Eq. (3.2). In this section, we consider three physically important cases.

A. Rectangular barrier potential

A rectangular barrier $V\theta_{ab}(x)$, with $V>0$, adds to the free-particle action a term

$$-\int_{t_1}^{t_2} V\theta_{ab}(x(t))dt=-Vt_{ab}^{\mathrm{cl}}[x(t)] .$$

Therefore from Eq. (3.6) we have

$$\eta_V(k,\tau)=\exp(-iV\tau/\hbar)\eta_0(k,\tau) \tag{6.1}$$

$$=\sum_{n=1}^{\infty}(-1)^{n-1}a_n\exp[i(W_n-V)\tau/\hbar] , \tag{6.2}$$

where $\eta_0(k,\tau)$ is the free-particle wave function discussed in Sec. IV and Eq. (4.6) has also been used.

It is instructive to examine how an increase in V affects $\eta_V(k,\tau)$ in the semiclassical limit $\beta\gg 1$. For $V=0$ it has been shown in Sec. IV that $\eta_0(k,\tau)$ has a stationary region around τ_0 of width $\Delta\tau\approx\tau_0/[2(2\beta)^{1/2}]$. For $\hbar/V\gg\Delta\tau$, the factor $\exp(-iV\tau/\hbar)$ oscillates slowly compared to $\Delta\tau$ and

$$\eta_V(k,\tau)\approx\exp(-iV\tau_0/\hbar)\eta_0(k,\tau) .$$

In physical terms, the barrier is too low to influence the particle's motion. A further increase in V results in a deformation and shift of the stationary region to larger times. As V approaches E, a simple classical picture no longer holds. In particular when

$$V\approx E-(\hbar\pi n)^2/[2m(b-a)^2] \quad \text{for } n=1,2,\ldots$$

we have, from Eq. (4.13), $\mathrm{Re}(W_n-V)\approx 0$, so that the oscillating contribution from the nth pole in Eq. (6.2) is absent. As shown in Sec. V, this behavior is typical of a resonance, resulting in complete transparency. Indeed, there is a well-known resonance effect discussed in Ref. [28] for energies near the top of a rectangular barrier. Finally, for $V\gg E$, the factor $\exp(-iV\tau/\hbar)$ oscillates rapidly, so that $\eta_V(k,\tau)$ no longer has a stationary region on the real τ axis. In particular, no unique real time, analogous to τ_0, can then be found for the tunneling particle. This point is analyzed further in Ref. [15].

The transmission amplitude $T_V(k)$ is obtained from Eqs. (3.2) and (6.2)

$$T_V(k)=i\hbar\sum_{n=1}^{\infty}(-1)^{n-1}\frac{a_n}{W_n-V} . \tag{6.3}$$

Since $T_V(k)\equiv 1$ for $V\equiv 0$, Eq.(6.3) yields the identity

$$i\hbar\sum_{n=1}^{\infty}(-1)^{n-1}a_n/W_n=1 . \tag{6.4}$$

Equations (6.3) and (6.4) let us write $T_V(k)$ in the alternative form

$$T_V(k)=T_{V\equiv 0}(k)+\sum_{n=1}^{\infty}R_n\left[\frac{1}{V-W_n}+\frac{1}{W_n}\right] , \tag{6.5}$$

where

$$R_n = \mathrm{Res}_n T(k,W) = i\hbar(-1)^n a_n, \quad n = 1,2,\ldots .$$

Equation (6.5) is an example of Mittag-Leffler's expansion theorem [29].

It is not difficult to show that $T_V(k)$ is a function of the dimensionless variables β and $\tilde{V} = V\tau_0/\hbar$. Figure 4 shows the transmission probability $P_V(k) = |T_V(k)|^2$ versus $\tilde{V}$ for $\beta = 6$.

Note that to calculate $T_V(k)$ from Eq. (6.1), we first need to know $T_0(k,W) \equiv T_W(k)$ for $-\infty < W < \infty$ in order to find $\eta_0(k,\tau)$; see Eq. (4.2). The next two examples are less circular.

B. Optical potential

A purely imaginary potential $-iU\theta_{ab}(x)$, with $U > 0$, describes absorption in $[a,b]$. It adds to the free-particle action a term

$$i\int_{t_1}^{t_2} U\theta_{ab}(x(t))dt = iUt_{ab}^{\mathrm{cl}}[x(t)]$$

so that

$$\eta_{\mathrm{opt}}(k,\tau) = \exp(-U\tau/\hbar)\eta_0(k,\tau)$$

and

$$T_{\mathrm{opt}}(k) = i\hbar\sum_{n=1}^{\infty}(-1)^{n-1}\frac{a_n}{W_n + iU} .$$

Unlike the previous case, the factor $\exp(-U\tau/\hbar)$ decreases monotonically with τ, which leads to a smooth monotonic decrease of the transmission probability $P_{\mathrm{opt}}(k) = |T_{\mathrm{opt}}(k)|^2$ with U. Figure 4 shows a plot of $P_{\mathrm{opt}}(k)$ versus the dimensionless variable $\tilde{U} = U\tau_0/\hbar$ for $\beta = 6$.

C. Interaction with a slow oscillator

Consider a free particle linearly coupled to an oscillator. The classical Hamiltonian for this system is

$$H = \frac{p^2}{2m} + \frac{P^2}{2M} + \frac{M\omega^2 Q^2}{2} + U(x)Q ,$$

where (m,p,x) and (M,P,Q) are the mass, momentum, and coordinate of the particle and oscillator, respectively. The transition amplitude for leaving the oscillator in its ground state can be written as a path integral with an effective action (Ref. [6], p. 233)

$$S[x(t)] = S_0[x(t)] + \frac{i}{2M\omega}\int_{t_1}^{t_2} dt \int_{t_1}^{t} ds\, U(x(t))U(x(s)) \times \exp[-i\omega(t-s)] , \quad (6.6)$$

where $S_0[x(t)]$ is the free-particle action. In general, the double integral in Eq. (6.6) cannot be expressed in terms of $t_{ab}^{\mathrm{cl}}[x(t)]$. However, in the special case $\omega \to 0$ and $U(x) = \lambda\theta_{ab}(x)$ we have

$$S[x(t)] = S_0[x(t)] + i\{\alpha t_{ab}^{\mathrm{cl}}[x(t)]\}^2 ,$$

where $\alpha = \lambda/(4M\omega)^{1/2}$.

The wave function $\eta_\alpha(k,\tau)$ becomes

$$\eta_\alpha(k,\tau) = \exp(-\alpha^2\tau^2/\hbar)\eta_0(k,\tau) . \quad (6.7)$$

Substituting Eqs. (4.6) and (6.7) into Eq. (3.2) allows the transmission amplitude $T_\alpha(k)$ to be written in terms of a sum of complementary error functions

$$T_\alpha(k) = \frac{(\pi\hbar)^{1/2}}{2\alpha}\sum_{n=1}^{\infty}(-1)^{n-1}a_n \exp\left[-\frac{W_n^2}{4\alpha^2\hbar}\right] \times \mathrm{erfc}\left[-\frac{iW_n}{2\alpha\hbar^{1/2}}\right] , \quad (6.8)$$

where

$$\mathrm{erfc}(z) = 1 - (2/\pi^{1/2})\int_0^z \exp(-t^2)dt .$$

Equation (6.8) can be rewritten in terms of the dimensionless variables β and $\tilde{\alpha} = \alpha\tau_0/\hbar^{1/2}$.

The factor $\exp(-\alpha^2\tau^2/\hbar)$ in Eq. (6.7) has a damping effect on $\eta_0(k,\tau)$. As a result, the transmission probability $P_\alpha(k) = |T_\alpha(k)|^2$ rapidly decreases for large α, in a similar way to $P_{\mathrm{opt}}(k)$. Figure 4 shows $P_\alpha(k)$ versus $\tilde{\alpha}^2$ for $\beta = 6$. The curves for $P_{\mathrm{opt}}(k)$ and $P_\alpha(k)$ have been plotted so that they would coincide in the classical limit $\eta_0(k,\tau) = \delta(\tau - \tau_0)$. The difference between the two curves in Fig. 4 is therefore a measure of the different Feynman paths which contribute to $T_{\mathrm{opt}}(k)$ and $T_\alpha(k)$.

Finally, we note that the method described in this section could be used to find $\eta(k,\tau)$ and $T(k)$ for any combination of the three interactions. We could also study the effect of the three interactions on resonance tunneling by replacing $\eta_0(k,\tau)$ with $\eta_{\delta\delta}(k,\tau)$ in the above equations.

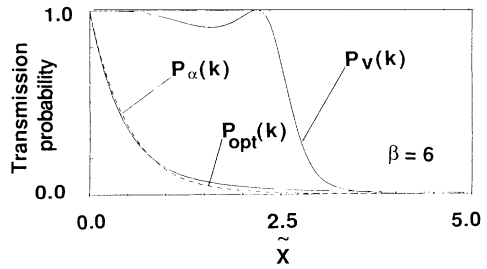

FIG. 4. Transmission probability at $\beta = 6$ versus $\tilde{X}$ for (a) a rectangular barrier, where $\tilde{X} = V\tau_0/\hbar$ (solid line); (b) for an optical potential, where $\tilde{X} = U\tau_0/\hbar$ (dashed line); and (c) for an interaction with a slow oscillator, where $\tilde{X} = \alpha^2\tau_0^2/\hbar$ (solid line).

VII. UNCERTAINTY RELATION AND MEASUREMENT OF THE TRAVERSAL TIME WITH A LARMOR CLOCK

In this section we first discuss an uncertainty relation for the traversal time. We then discuss measurement of the traversal time using a Larmor clock, which we apply to free-particle motion, a rectangular barrier, and resonance tunneling.

A. Uncertainty relation

It is well known (Ref.[23], p. 130) that the Fourier transform relation (2.4) between $\eta(f)$ and $g(\lambda)$ implies a Heisenberg-type uncertainty relation $\Delta f \Delta\lambda \gtrsim \hbar$, where $\eta(f)$ is assumed to occupy a region of order Δf in f space and $g(\lambda)$ is assumed to occupy a region of order $\Delta\lambda$ in λ space. It follows from this uncertainty relation that f and λ cannot both be known simultaneously.

In a similar way, for the traversal wave function (3.1) we can write

$$\Delta\tau \Delta W \gtrsim \hbar \ , \tag{7.1}$$

Now $T(k,W)$ in Eq. (3.1) is the transmission amplitude for the composite potential $V(x)+W\theta_{ab}(x)$. A measurement of the traversal time to an accuracy of $\Delta\tau$ therefore results in an uncertainty of $\Delta W \gtrsim \hbar/\Delta\tau$ in the composite potential. Since $V(x)$ is fixed, we conclude that this uncertainty must be introduced by the measuring device. A different uncertainty relation has been discussed in Refs. [18,19].

B. Larmor clock

The traversal time can be measured by a Larmor clock [1,30–33]. This consists of a spin with $2j+1$ components, $j=\frac{1}{2},1,\frac{3}{2},\ldots$, which interacts with a uniform magnetic field H directed along the z axis, when the particle is inside $[a,b]$. Following Peres [32] and Foden and Stevens [33] (PFS), we describe the clock using orthonormal states $|\gamma^k\rangle$, $k=0,1,2,\ldots,2j$, with

$$|\gamma^k\rangle = \sum_{m=-j}^{j} \gamma_m^k |m\rangle, \quad k=0,1,2,\ldots,2j \tag{7.2}$$

where

$$\gamma_m^k \equiv \langle m|\gamma^k\rangle = (2j+1)^{-1/2}\exp(-im\phi_k^{(j)}) \ , \qquad k=0,1,2,\ldots,2j \tag{7.3}$$

and the rotation angle $\phi_k^{(j)}$ is

$$\phi_k^{(j)} = 2\pi k/(2j+1), \quad k=0,1,2,\ldots,2j \ . \tag{7.4}$$

The number m is the projection quantum number along the direction of the magnetic field. The clock described by Eqs. (7.2)–(7.4) is shown schematically in Fig. 5.

If the spin is in the state $|\gamma^0\rangle$ prior to collision, the probability amplitude to find the spin in the state $|\gamma^k\rangle$ after the collision is [from Eqs. (10) and (13) of Ref. [14]]

$$\Psi(E,\phi_k^{(j)}) = \int_0^\infty G^{\mathrm{PFS}}(\phi_k^{(j)}-\omega\tau)\eta(E,\tau)d\tau \ , \qquad k=0,1,2,\ldots,2j \tag{7.5}$$

where ω is the Larmor angular velocity and

$$G^{\mathrm{PFS}}(y) = (2j+1)^{-1}\sum_{m=-j}^{j}\exp(imy) \tag{7.6}$$

$$= (2j+1)^{-1}\frac{\sin[(2j+1)y/2]}{\sin(y/2)} \ . \tag{7.7}$$

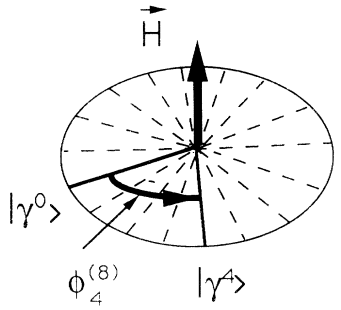

FIG. 5. Schematic representation of the basis set $|\gamma^k\rangle$ with $k=0,1,2,\ldots,2j$ used to describe a Larmor clock. The rotation angle $\phi_k^{(j)}$ for $k=4$ and $j=8$ is illustrated.

For large j, the factor $G^{\mathrm{PFS}}(\phi_k^{(j)}-\omega\tau)$, as a function of τ, has sharp peaks near $\tau=\mathcal{T}_k^{(j,n)}\equiv[\phi_k^{(j)}+2\pi n]/\omega$ with $n=0,\pm1,\pm2,\ldots$ (see Fig. 1 of Ref. [14]). The base width of the peaks, which determines the accuracy (resolution) of the measurement, is approximately

$$R_j = 4\pi/[(2j+1)\omega] \ . \tag{7.8}$$

Next, we choose the Larmor period $T_L=2\pi/\omega$ to be large compared to the time scale on which $\eta(E,\tau)$ vanishes as a function of τ, i.e., $T_L \gg \tau_{\max}$. Then only the $n=0$ peak of $G^{\mathrm{PFS}}(\phi_k^{(j)}-\omega\tau)$ contributes to $\Psi(E,\phi_k^{(j)})$ and comparing Eq. (7.5) with Eq. (3.3) we see that rotation of the spin through the angle $\phi_k^{(j)}$ is equivalent to a traversal time for the particle in $[a,b]$ of

$$\mathcal{T}_k^{(j)} \equiv \mathcal{T}_k^{(j,0)} \approx \phi_k^{(j)}/\omega, \quad k=0,1,2,\ldots,2j \ .$$

Equation (7.8) shows that the uncertainty R_j in $\mathcal{T}_k^{(j)}$ decreases as j and ω increase. Note that for $k=0$, we have $\mathcal{T}_0^{(j)}\approx 0$. One might be tempted to conclude that passage through $[a,b]$ is then an infinitely fast process. However, the finite uncertainty for R_j prevents us from changing $\mathcal{T}_0^{(j)}\approx 0$ to $\mathcal{T}_0^{(j)}\equiv 0$. We examine the limit $R_j\to 0$ in Sec. VIII.

We can use the analysis just presented to verify the uncertainty relation (7.1). For the initial state $|\gamma^0\rangle$, Eqs. (7.2)–(7.4) give

$$|\gamma^0\rangle = (2j+1)^{-1/2}\sum_{m=-j}^{j}|m\rangle \ ,$$

i.e., the states $|m\rangle$ are uniformly distributed between $|-j\rangle$ and $|j\rangle$. Next we note that if the spin is in state $|m\rangle$, the particle encounters an additional potential $\hbar m\omega\theta_{ab}(x)$ [31]. Thus the uncertainty in the scattering potential is $\Delta W \approx 2\hbar j\omega$. We also know that $\Delta\tau \approx R_j \approx 4\pi/[(2j+1)\omega]$. Constructing the product of $\Delta\tau$ with ΔW gives $\Delta\tau W \approx 4\pi\hbar$, in accordance with the uncertainty relation (7.1).

C. Measurement of the traversal time

We now consider the measurement of the traversal time by the Larmor clock method for three choices of the potential $V(x)$. We assume the clock is set as in Sec. VII B so that Eqs. (7.2)–(7.7) apply. The experiment con-

sists of particles with energy E and a large spin quantum number, $j \gg 1$, impinging on $V(x)$ from the left. Particles are then detected on the right-hand side of the potential, and the angle of spin rotation in the plane perpendicular to the magnetic field $\phi_k^{(j)}$, with $k=0,1,2,\ldots,2j$, is determined. Finally, the traversal time $\mathcal{T}_k^{(j)} \approx \phi_k^{(j)}/\omega$ is calculated for each k. The measured values $\{\mathcal{T}_k^{(j)}\}$ are discrete, but can be approximated by a continuous distribution for $j \gg 1$.

The normalized probability distribution for the measured values of the traversal time is, by definition,

$$P(E,\mathcal{T}_k^{(j)}) = |\Psi(E,\phi_k^{(j)})|^2 \Big/ \sum_{k=0}^{2j} |\Psi(E,\phi_k^{(j)})|^2 , \quad k=0,1,2,\ldots,2j . \tag{7.9}$$

We can evaluate $\Psi(E,\phi_k^{(j)})$ by first replacing the lower limit of the integral (7.5) by $-\infty$ [which is allowed, since $\eta(E,\tau)\equiv 0$ for $\tau<0$] and then inserting Eqs. (3.1) and (7.6). The resulting series simplifies to

$$\Psi(E,\phi_k^{(j)}) = (2j+1)^{-1} \sum_{m=-j}^{j} T(E,m\hbar\omega)\exp(im\phi_k^{(j)}) , \quad k=0,1,2,\ldots,2j . \tag{7.10}$$

We also find that

$$\sum_{k=0}^{2j} |\Psi(E,\phi_k^{(j)})|^2 = (2j+1)^{-1} \sum_{m=-j}^{j} |T(E,m\hbar\omega)|^2 . \tag{7.11}$$

We now use Eqs. (7.9)–(7.11) to calculate $P(E,\mathcal{T}_k^{(j)})$ for the three potentials discussed in Secs. IV, V, and VI A.

1. Free motion

We have evaluated $P(E,\mathcal{T}_k^{(j)})$ for $j=20$ and forty-one values of k in the range from 0 to 40 for $T_L = 2\tau_0$ (i.e., $R_j \approx 0.1\tau_0$). The perspective plot in Fig. 6 shows P vs $\mathcal{T}_k^{(j)}/\tau_0$ for $k=0,1,2,\ldots,2j$ and the dimensionless variable $\beta \equiv k(b-a)$ (here k is the wave number) with $0.001 \le \beta \le 450$.

For $\beta \approx 450$, the semiclassical peak at $\mathcal{T}_k^{(j)}/\tau_0 \approx 1$ is clearly visible. As β becomes smaller, this peak broadens and breaks up into smaller multiple peaks. For the smallest value of β shown in the plot, $\beta = 0.001$, the Larmor clock reading is distributed exponentially as predicted by Eq. (4.12).

2. Rectangular barrier

An analogous plot of $P(E,\mathcal{T}_k^{(j)})$ for a rectangular barrier potential with $(2mV)^{1/2}(b-a)/\hbar = 150$ is shown in Fig. 7. For $\beta \approx 450$, i.e., for E much greater than V, there is a well-defined semiclassical peak similar to the free particle one. The peak is almost completely destroyed for $E \approx V$ (i.e., $\beta \approx 150$) in the resonance region near the barrier top that was mentioned in Sec. VI A.

In the tunneling regime $\beta \le 150$, we find that the clock is essentially nonzero only for $\mathcal{T}_0^{(j)} = 0$. (Note that the plot has been reduced by a factor of 10 for $\beta \le 112.5$ and $k=0$ in this case to allow for better viewing.) The dominance of $k=0$ in the $P(E,\mathcal{T}_k^{(j)})$ distribution occurs because (a) the highly oscillatory nature of $\eta_V(E,\tau)$ for $E \ll V$ [see the discussion following Eq. (6.2)] implies that the main contribution to the integral (7.5) for $\Psi(E,\phi_k^{(j)})$ comes from the region close to the endpoint $\tau=0$ and (b) the function $G^{\mathrm{PFS}}(\phi_k^{(j)}-\omega\tau)$ has a sharp peak at $\tau=0$ for $k=0$.

3. Resonance tunneling

In Sec. V C we showed that for $\chi \gg \beta$, the time delay associated with the well when $E \approx E_l$ can be observed, provided the nonoscillatory tail $-(\frac{1}{2}\Gamma_l/\hbar)\exp(-\frac{1}{2}\Gamma_l\tau/\hbar)$ can be isolated from the rapidly oscillating terms in the series (5.7) for $\eta_{\delta\delta}(E,\tau)$. In particular, if we choose $\tau_0 \ll R_j \ll \hbar/\frac{1}{2}\Gamma_l$ we might expect the Larmor clock for $E \approx E_l$ to produce readings at large values of $\mathcal{T}_k^{(j)}$, while off resonance the readings should be grouped around $\mathcal{T}_0^{(j)}$.

Figure 8 shows $P(\chi;E,\mathcal{T}_k^{(j)})$ for $j=20$, $\chi=600$, and

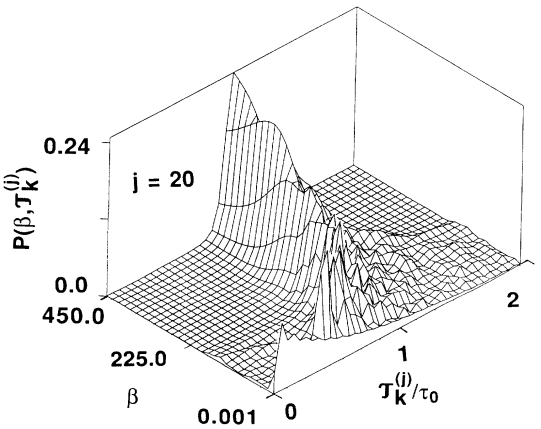

FIG. 6. Perspective plot of the probability $P(\beta,\mathcal{T}_k^{(j)})$ for free motion versus β and $\mathcal{T}_k^{(j)}/\tau_0$ for $k=0,1,2,\ldots,2j$ with $j=20$ and $T_L = 2\tau_0$ ($R_j \approx 0.1\tau_0$).

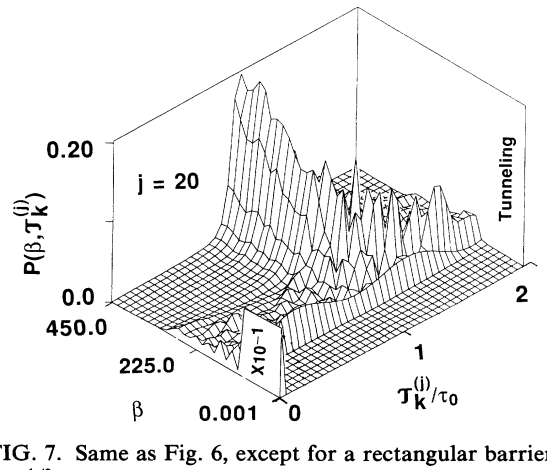

FIG. 7. Same as Fig. 6, except for a rectangular barrier with $(2mV)^{1/2}(b-a)/\hbar = 150$. The plot has been reduced by a factor of 10 for $k=0$ (i.e., for $\mathcal{T}_0^{(j)}/\tau_0 = 0$) and $0.001 \le \beta \le 112.5$ to allow for better viewing.

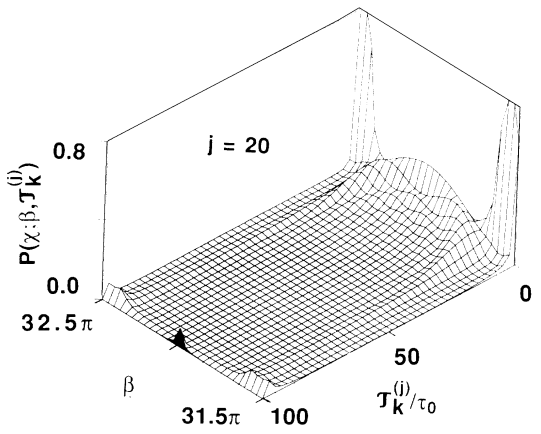

FIG. 8. Same as Fig. 6, except for the double-δ-function potential with $j=20$, $\chi=600$, and $T_L=100\tau_0$ ($R_j\approx 5\tau_0$). The approximate position of the resonance at $\beta=32\pi$ is indicated by a black triangle.

$T_L=100\tau_0$ (i.e., $R_j\approx 5\tau_0$), with $31.5\pi\leq\beta\leq 32.5\pi$, which includes the 32nd resonance at $\beta_{32}\approx 32\pi$; the lifetime of this resonance is $\hbar/\frac{1}{2}\Gamma_{32}\approx 17.8\tau_0$. The effect of the resonance can be seen clearly in Fig. 8; there are also large peaks at $k=0$, corresponding to "fast" off-resonance tunneling. The small bumps at $\mathcal{T}_k^{(j)}/\tau_0\approx 100$ come from the overlap in Eq. (7.5) of the peaks in $G^{\rm PFS}(\phi_k^{(j)}-\omega\tau)$ for $k=38-40$ (which are centered at small negative values of τ) with $\eta_{\delta\delta}(E,\tau)$.

Figure 9 shows a similar plot to Fig. 8 except that now we have improved the resolution R_j by setting $j=250$ so that $R_j\approx 0.4\tau_0$. The peaks in $P(\chi;E,\mathcal{T}_k^{(j)})$ at $\mathcal{T}_k^{(j)}/\tau_0\approx 1,3,5$ correspond to the particle crossing $[a,b]$ once, three times after two reflections, and five times after four reflections, respectively. The peaks become broader and more distorted as $\mathcal{T}_k^{(j)}/\tau_0$ increases. To resolve peaks for six or more reflections would require calculations be carried out for larger values of the semiclassical parameter β. Note there is very little change in the plot on passing through the resonance. Thus observation of the resonance lifetime (Fig. 8) and multiple bounces in the well (Fig. 9) requires different resolutions—they are not both seen simultaneously.

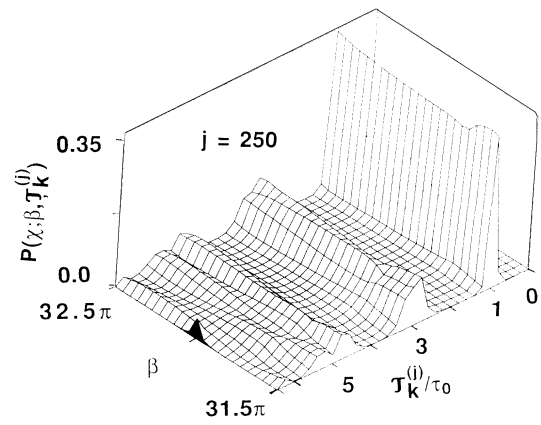

FIG. 9. Same as Fig. 6, except for the double-δ-function potential with $j=250$, $\chi=600$, and $T_L=100\tau_0$ ($R_j\approx 0.4\tau_0$). The approximate position of the resonance at $\beta=32\pi$ is indicated by a black triangle.

In summary, by adjusting the resolution R_j of the Larmor clock, we have been able to obtain readings that are consistent with different pictures used to describe resonance tunneling. In the next section, we study the limit in which the clock tends to infinite accuracy, $R_j\rightarrow 0$, i.e., an ideal measurement of the traversal time.

VIII. HIGH-RESOLUTION LIMIT OF A TRAVERSAL-TIME MEASUREMENT

A. Introduction

Consider Eq. (3.3) applied to an infinitely accurate (ideal) measurement of a quantity x (e.g., the coordinate of a particle), which is described by a wave function $\phi(x)$. For this situation, the apparatus function must be $G(X,x)=\delta(X-x)$. It then follows that the normalized probability $W(X,X+\delta X)$ for the result of an ideal measurement to lie in the interval $[X,X+dX]$ is given by the standard result

$$W(X,X+\delta X)=\int_X^{X+\delta X}|\phi(x)|^2dx\Big/\int_{-\infty}^{\infty}|\phi(x)|^2dx\ . \tag{8.1}$$

The same argument cannot be applied directly to the traversal time because the integral $\int_0^\infty|\eta(E,\tau)|^2d\tau$ is divergent, as has been discussed in Sec. IV B for the free-particle case. However, we will show that this divergence is also present in the numerator and the corresponding normalized probability $W(\mathcal{T},\mathcal{T}+\delta\mathcal{T})$ is a well-defined quantity.

B. High-resolution limit of a Larmor clock measurement

We consider, as discussed in the preceding section, a Larmor clock measurement of the traversal time for a free particle. The normalized probability $W_j(\mathcal{T},\mathcal{T}+\delta\mathcal{T})$ for the result of a measurement to lie in the time interval $[\mathcal{T},\mathcal{T}+\delta\mathcal{T}]$ at an energy E is, by definition,

$$W_j(\mathcal{T},\mathcal{T}+\delta\mathcal{T})\equiv\sum_{k=0}^{2j}\theta_{\mathcal{T},\mathcal{T}+\delta\mathcal{T}}(\mathcal{T}_k^{(j)})P(E,\mathcal{T}_k^{(j)})\ ,$$

where $P(E,\mathcal{T}_k^{(j)})$ is given by Eq. (7.9). We will assume that $j\gg 1$ and that many k states lie in the interval $\delta\mathcal{T}$.

In order to isolate the divergence of $\eta_0(E,\tau)$ we introduce a truncated wave function $\eta_0^N(E,\tau)$, which contains only the first N terms of the residue sum (4.6):

$$\eta_0^N(E,\tau)\equiv\sum_{n=1}^{N}(-1)^{n-1}a_n\exp(iW_n\tau/\hbar)$$

so that

$$\eta_0(E,\tau)=\lim_{N\rightarrow\infty}\eta_0^N(E,\tau)\ .$$

Replacing $\eta_0(E,\tau)$ by $\eta_0^N(E,\tau)$ in Eqs. (7.5) and (7.9) yields the approximate probabilities $P^N(E,\mathcal{T}_k^{(j)})$ and $W_j^N(\mathcal{T},\mathcal{T}+\delta\mathcal{T})$

$$W_j^N(\mathcal{T},\mathcal{T}+\delta\mathcal{T})\equiv\sum_{k=0}^{2j}\theta_{\mathcal{T},\mathcal{T}+\delta\mathcal{T}}(\mathcal{T}_k^{(j)})P^N(E,\mathcal{T}_k^{(j)})\ . \quad (8.2)$$

Now the high-resolution limit $R_j\to 0$ corresponds to $j\to\infty$, so the probability $W(\mathcal{T},\mathcal{T}+\delta\mathcal{T})$ can be written

$$W(\mathcal{T},\mathcal{T}+\delta\mathcal{T})=\lim_{\substack{j\to\infty\\N\to\infty}} W_j^N(\mathcal{T},\mathcal{T}+\delta\mathcal{T})\ . \quad (8.3)$$

It is convenient to consider first the limit $j\to\infty$ in Eq. (8.3). From Eq. (7.7) we have (for the $n=0$ peak)

$$\lim_{j\to\infty} G^{\mathrm{PFS}}(\phi_k^{(j)}-\omega\tau)=\frac{2\pi}{(2j+1)\omega}\delta(\tau-\mathcal{T}_k^{(j)})\ ,$$
$$k=0,1,2,\ldots,2j\ . \quad (8.4)$$

We also recall from Sec. VII B that retaining only the $n=0$ peak implies $T_L\gg\tau_{\max}$. Inserting Eq. (8.4) into Eq. (7.5) and replacing the sum in the denominator of Eq. (7.9) by an integral, we find

$$\lim_{j\to\infty} P^N(E,\mathcal{T}_k^{(j)})=\frac{2\pi}{(2j+1)\omega}\frac{|\eta_0^N(E,\mathcal{T}_k^{(j)})|^2}{\int_0^\infty|\eta_0^N(E,\tau)|^2d\tau}\ ,$$
$$k=0,1,2,\ldots,2j\ . \quad (8.5)$$

Finally, substituting Eq. (8.5) into Eq. (8.2) and replacing the sum in Eq. (8.2) by an integral, we obtain for Eq. (8.3) the result

$$W(\mathcal{T},\mathcal{T}+\delta\mathcal{T})=\lim_{N\to\infty}\int_{\mathcal{T}}^{\mathcal{T}+\delta\mathcal{T}}|\eta_0^N(E,\tau)|^2d\tau\Big/\int_0^\infty|\eta_0^N(E,\tau)|^2d\tau\ . \quad (8.6)$$

Equation (8.6) is the analog of Eq. (8.1).

Next we consider the $N\to\infty$ limit of Eq. (8.6). According to Eq. (4.6), $|\eta_0^N(E,\tau)|^2$ consists of a double sum. A more detailed analysis shows that the divergence of the integrals in Eq. (8.6) arises from the diagonal terms in this sum, i.e., we can replace $|\eta_0^N(E,\tau)|^2$ by

$$\sum_{n=1}^{N}|a_n|^2\exp(-2\,\mathrm{Im}W_n\tau/\hbar)\ .$$

Equations (4.8) and (4.9) tell us that for $n\to\infty$, we have $\mathrm{Im}W_n\to 2\hbar/\tau_0$ and $|a_n|^2\to 4/\tau_0^2$, so that

$$\lim_{N\to\infty}\sum_{n=1}^{N}|a_n|^2\exp(-2\,\mathrm{Im}W_n\tau/\hbar)=N\frac{4}{\tau_0^2}\exp(-4\tau/\tau_0)\ . \quad (8.7)$$

After using the result Eq. (8.7) in Eq. (8.6), we find that the factor N in the numerator and denominator cancels and that a high-resolution (ideal) measurement of the traversal time is distributed exponentially with a lifetime of $\tau_0/4$:

$$W(\mathcal{T},\mathcal{T}+\delta\mathcal{T})=\frac{4}{\tau_0}\exp(-4\mathcal{T}/\tau_0)\delta\mathcal{T}\ . \quad (8.8)$$

The derivation of Eq. (8.8) has assumed that $R_j\ll\delta\mathcal{T}\ll\tau_0$.

As a check on the validity of Eq. (8.8) we have simulated a high-resolution measurement of the traversal time in the following way. First we set $T_L\gg\tau_0/4$ and then split the interval $[0,T_L]$ into I subintervals of width $\delta\mathcal{T}=T_L/I$. We then evaluated Eq. (8.2) for a fixed $j\gg 1$ in each subinterval $[\mathcal{T}_i,\mathcal{T}_i+\delta\mathcal{T}]$ with $i=0,1,2,\ldots,I-1$.

Figure 10 shows the results for $T_L=2\tau_0$, $I=50$ (corresponding to $\delta\mathcal{T}=0.04\tau_0$), and $\beta=5$. Plots for two values of j are shown, namely, $j=100$ (i.e., $R_j\approx 0.02\tau_0$) and $j=1000$ (i.e., $R_j\approx 0.002\tau_0$). In both cases, 900 poles have been retained in the residue sum. Also plotted in Fig. 10 is the exponential distribution of Eq. (8.8). As R_j decreases, it can be seen that the distribution of measured traversal times does indeed tend to the limit (8.8). Note that the number of terms N required in the residue sum is $O(j^{1/2})$; see Eq. (8.12). The analysis presented above also applies to a rectangular barrier because $\eta_V(E,\tau)$ only differs from $\eta_0(E,\tau)$ by the factor $\exp(-iV\tau/\hbar)$; see Eq. (6.1).

C. Quenching of transmission by an accurate clock

Finally, we consider the total transmission probability for a free particle in the presence of a Larmor clock, which is given by the sum in the denominator of Eq. (7.9), namely,

$$P_{\mathrm{clock}}(E,j)=\sum_{k=0}^{2j}|\Psi(E,\phi_k^{(j)})|^2\ . \quad (8.9)$$

To estimate $P_{\mathrm{clock}}(E,j)$, we again replace $\eta_0(E,\tau)$ by $\eta_0^N(E,\tau)$ and then take the limits $j\to\infty$ and $N\to\infty$. The resulting sum for $P_{\mathrm{clock}}^N(E,j)$ has already been evaluated in the derivation of Eq. (8.5). We have

$$\lim_{j\to\infty} P_{\mathrm{clock}}^N(E,j)=\frac{2\pi}{(2j+1)\omega}\int_0^\infty|\eta_0^N(E,\tau)|^2d\tau \quad (8.10)$$

and with the help of Eq. (8.7)

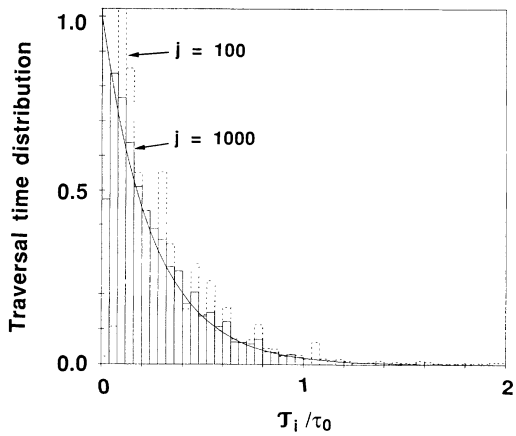

FIG. 10. Histogram of $\tau_0 W_j^N(\mathcal{T}_i,\mathcal{T}_i+\delta\mathcal{T})/(4\delta\mathcal{T})$ for free motion versus $\mathcal{T}_i/\tau_0$ with $i=0,1,2,\ldots,49$, $\delta\mathcal{T}=0.04\tau_0$, $T_L=2\tau_0$, $\beta=5$, and $N=900$, for (a) $j=100$, corresponding to $R_j\approx 0.02\tau_0$ (dashed lines) and (b) $j=1000$, corresponding to $R_j\approx 0.002\tau_0$ (solid lines). The solid curve shows the high-resolution limiting result $\exp(-4\mathcal{T}/\tau_0)$.

$$\lim_{\substack{j\to\infty \\ N\to\infty}} P^N_{\text{clock}}(E,j)=\frac{2\pi N}{(2j+1)\omega\tau_0} . \tag{8.11}$$

Next we estimate the number of terms N in the residue sum which contribute to the integral (7.5) by noting that the period of oscillation of $\exp(iW_n\tau/\hbar)$ for $n\gg 1$ decreases as $1/n^2$; see Eq. (4.8). Equating the period to the base width of (the $n=0$ peak in) $G^{\text{PFS}}(\phi_k^{(j)}-\omega\tau)$ gives an estimate for N. From Eq. (7.8) we have

$$\frac{2\pi\hbar}{|W_N|}\approx\frac{4\pi}{(2j+1)\omega}$$

and using Eq. (4.8) we obtain

$$N\approx\left[\frac{2mj\omega}{\hbar}\right]^{1/2}\frac{(b-a)}{\pi} . \tag{8.12}$$

In Eq. (8.12), m is the mass of the particle. Using Eq. (8.12) in Eq. (8.11) shows that $P_{\text{clock}}(E,j)$ is $O(1/j^{1/2})$, i.e., a highly accurate Larmor clock ($j\gg 1$) will lead to reflection of almost all the particles incident on the interval $[a,b]$. This is an inevitable consequence of the distortion of the particle's motion by the measuring device.

Note the result (8.8) gives the normalized conditional probability $W(\mathcal{T},\mathcal{T}+\delta\mathcal{T})$ that the particle has crossed $[a,b]$, i.e., Larmor clock readings for the transmitted particle. Although the clock strongly perturbs the motion of the particle, also note that the result (8.7), as well as the wave function $\eta_0(E,\tau)$ used to obtain it, are for the unperturbed motion without the clock [14].

IX. TRAVERSAL-TIME ANALYSIS AND THE USE OF "FAST" AND "SLOW" IN QUANTUM MECHANICS

A. Introduction

A great deal of practical interest in quantum traversal times, and in particular tunneling times, arises from the hope of finding quantum time scales analogous to those in classical mechanics. Once discovered, these scales are thought to tell one whether the scattering is fast or slow, thereby justifying sudden or adiabatic approximations for scattering problems in which a particle interacts with an external time-dependent field or with other degrees of freedom [1].

The use of a quantum time scale would typically involve three steps. First, the exact action $S[x(t)]$ for the problem would be replaced by an approximate one $S_0[x(t)]$, for which a solution of the Schrödinger equation could be obtained more easily. Second, a quantum traversal time would be found for the motion of the particle governed by $S_0[x(t)]$ through $[a,b]$. Third, neglect of the remainder $\Delta S[x(t)]$ in

$$S[x(t)]=S_0[x(t)]+\Delta S[x(t)]$$

would be justified on the grounds that the particle spends in $[a,b]$ a (real) duration which is short (i.e., fast) or long (i.e., slow) compared to a characteristic time associated with the external time-dependent field or other degrees of freedom.

We now examine how these three steps might be implemented using the traversal-time wave function.

B. Interactions expressed in terms of $t_{ab}^{\text{cl}}[x(t)]$

Let us assume that

$$\Delta S[x(t)]=f(t_{ab}^{\text{cl}}[x(t)]) , \tag{9.1}$$

where f an arbitrary function of $t_{ab}^{\text{cl}}[x(t)]$. In general, no unique traversal time is available for the motion governed by $S_0[x(t)]$; rather there is a distribution of times and in the second step we must use the wave function $\eta_0(k,\tau)$. In order to carry out the third step, we express the exact and approximate transmission amplitudes $T(k)$ and $T_0(k)$, respectively, in terms of $\eta_0(k,\tau)$:

$$T(k)=\int_0^\infty \exp[if(\tau)/\hbar]\eta_0(\tau)d\tau \tag{9.2}$$

and

$$T_0(k)=\int_0^\infty \eta_0(\tau)d\tau , \tag{9.3}$$

where Eqs. (3.2) and (3.6) have been used. We then ask the following question: Under what conditions does $T(k)\approx T_0(k)$, so that the replacement of $S[x(t)]$ by $S_0[x(t)]$ is permissible?

C. (Semi)classical examples

We first consider the (semi)classical limit $\eta_0(\tau)=\delta(\tau-\tau^{\text{cl}})$, where τ^{cl} is the classical traversal time for motion through $[a,b]$ (see Sec. IV B (iv) (c) and Ref. [15]). For $T(k)\approx T_0(k)$, Eqs. (9.2) and (9.3) show that we must have $\exp[if(\tau^{\text{cl}})/\hbar]\approx 1$ or, equivalently, $|f(\tau^{\text{cl}})|/\hbar\ll 1$.

Figure 11 illlustrates schematically two situations which can arise. For $f=f_{\text{slow}}(\tau)$, the exponent f is nonzero only for long (slow) times $\tau>\tau^{\text{cl}}$. As a result we have $T(k)=T_0(k)$ and can neglect $\Delta S[x(t)]$. Alternatively, for $f=f_{\text{fast}}(\tau)$, the exponent is large for short (fast) times $0\le\tau<\tau^{\text{cl}}$, but vanishes for $\tau\gtrsim\tau^{\text{cl}}$, i.e., $\Delta S[x(t)]$ does not have any effect on $T(k)$.

Another possibility is $f=f_{\text{slow}}(\tau)+f_{\text{fast}}(\tau)$, where again $T(k)=T_0(k)$, although a simple "fast" or "slow" argument does not apply in this case.

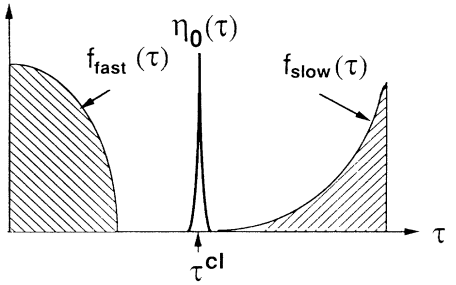

FIG. 11. Schematic representation of $\eta_0(\tau)=\delta(\tau-\tau^{\text{cl}})$ and a "fast" and "slow" $f(\tau)$, as used in the analysis of the transmission amplitude.

D. Quantum examples

In the quantum case, $\mathrm{Re}\eta_0(\tau)$ and $\mathrm{Im}\eta_0(\tau)$ typically have finite extent along the τ axis and there exists a $\tau_{\max}$ such that $\eta_0(\tau)\approx 0$ for $\tau \gtrsim \tau_{\max}$. The slow example discussed above can always be realized by choosing $f(\tau)$ (assumed to be real) to be nonzero only for $\tau \gtrsim \tau_{\max}$.

Another example of a slow interaction is the free-particle plus slow oscillator, which was discussed in Sec. VI C. In the (ultra)quantum limit $\beta \ll 1$, we have, from Eq. (4.12), $\eta_0(\tau)\approx \tau_0^{-1}\exp(-\tau/\tau_0)$ and from Eq. (6.7), $f(\tau)=i\alpha^2\tau^2$ with $\alpha>0$. In order to have $T(k)\approx T_0(k)$, we must have $\alpha \ll \hbar^{1/2}/\tau_0$, so that the exponential $\exp(-\alpha^2\tau^2/\hbar)$ in Eq. (9.2) is approximately unity. In this case, a traversal-time analysis with a slow $f(\tau)$ has led to a restriction on the value of α. Equivalently, we have arrived at the condition for the interaction to be sufficiently small to be treated perturbatively. Note that expanding the exponent in Eq. (9.2) yields a perturbation series in the coupling constant.

Since $\eta_0(\tau)=\tau_0^{-1}\exp(-\tau/\tau_0)$ decreases monotonically from $\tau=0$, it is easy to see that in general we cannot argue that there is a $f(\tau)$ which is very fast and hence negligible. Instead, any slowly varying $f(\tau)$, which takes significant values between 0 and τ_0, will contribute to the integral (9.2) and change the transmission amplitude.

E. An additional ambiguity

An additional ambiguity arises if we are only interested in the transmission probability $|T(k)|^2$ rather than $T(k)$ itself. It is possible for the interaction $\Delta S[x(t)]$ to change the phase of $T(k)$, but leave its modulus unchanged. In this situation, one should analyze the double integral

$$|T(k)|^2=\int_0^\infty d\tau\int_0^\infty d\tau' \exp\{i[f(\tau)-f^*(\tau')]/\hbar\} \times \eta_0(\tau)\eta_0^*(\tau')$$

rather than the single integral (9.2)

Throughout this section, we have assumed that $\Delta S[x(t)]$ is expressed in terms of $t_{ab}^{\mathrm{cl}}[x(t)]$. We briefly discuss the case when Eq. (9.1) does not apply in the next section.

X. TRAVERSAL-TIME ANALYSIS FOR MORE GENERAL INTERACTIONS

A. Introduction

This section discusses the difficulties that arise when $\Delta S[x(t)]\neq f(t_{ab}^{\mathrm{cl}}[x(t)])$. As a concrete example, we will consider a rectangular barrier whose height increases linearly with time,

$$V(x,t)=(V+ut)\theta_{ab}(x) , \tag{10.1}$$

where $u>0$.

Consider a quantum particle impinging on the time-dependent barrier (10.1). A classical analogy suggests that the particle will "see" a static barrier if the duration spent inside $[a,b]$ is sufficiently short. We will show, however, that a simple criterion for the validity of this sudden approximation does not follow from the analysis of the preceding section, because the problem requires a different functional than $t_{ab}^{\mathrm{cl}}[x(t)]$.

B. Traversal-time analysis

The action for the system (10.1) can be written in the form

$$S[x(t)]=S_V[x(t)]-u\int_{t_1}^{t_2} t\theta_{ab}(x(t))dt . \tag{10.2}$$

Following the development of the theory in Sec. II, we define a traversal-time wave function by

$$\eta(\tau)=\int_{x_1,t_1}^{x_2,t_2} Dx(\cdot)\delta(t_{ab}^{\mathrm{cl}}[x(\cdot)]-\tau)\exp\{iS[x(\cdot)]/\hbar\} ,$$

where for simplicity Ψ_1 and Ψ_2 in Eq. (2.2) are chosen to be Dirac δ functions. From Eq. (2.3), we have for the transition amplitude

$$g(x_2,t_2|x_1,t_1)=\int_{t_1}^{t_2}\eta(\tau)d\tau . \tag{10.3}$$

Next we rewrite Eq. (10.3) in the form [cf. Eq. (3.5)]

$$g(x_2,t_2|x_1,t_1)=\int_{t_1}^{t_2} A(\tau)\eta_V(\tau)d\tau ,$$

where

$$A(\tau)=\eta(\tau)/\eta_V(\tau)$$

with

$$\eta_V(\tau)=\int_{x_1,t_1}^{x_2,t_2} Dx(\cdot)\delta(t_{ab}^{\mathrm{cl}}[x(\cdot)]-\tau)\exp\{iS_V[x(\cdot)]/\hbar\} .$$

Unfortunately no further simplification of $A(\tau)$ is possible to give a result analogous to Eq. (3.6) or (9.2), which formed the starting point for the traversal-time analysis of Sec. IX. The reason is that the value of

$$t_{ab}^{\mathrm{cl}}[x(t)]\equiv\int_{t_1}^{t_2}\theta_{ab}(x(t))dt$$

does not uniquely define the value of the functional

$$\Theta_{ab}^{\mathrm{cl}}[x(t)]\equiv\int_{t_1}^{t_2} t\theta_{ab}(x(t))dt ,$$

which enters in Eq. (10.2). To see this, consider two paths which both cross $[a,b]$ once. Let us assume that they enter and leave $[a,b]$ at times $T_1, T_1+\tau$ and $T_2, T_2+\tau$, respectively. The value of $t_{ab}^{\mathrm{cl}}[x(t)]$ is τ for both paths, whereas the value of $\Theta_{ab}^{\mathrm{cl}}[x(t)]$ is $\tau(\tau+2T_1)/2$ for the first path and $\tau(\tau+2T_2)/2$ for the second one.

C. Analysis in terms of the functional $\Theta_{ab}^{\mathrm{cl}}[x(t)]$

The discussion of Sec. X B suggests that the appropriate variable for the problem is $\Theta_{ab}^{\mathrm{cl}}[x(t)]$ rather than $t_{ab}^{\mathrm{cl}}[x(t)]$. To this end, we define wave functions in the representation of $\Theta_{ab}^{\mathrm{cl}}[x(t)]$ by

$$\chi(\theta)=\int_{x_1,t_1}^{x_2,t_2} Dx(\cdot)\delta(\Theta_{ab}^{\mathrm{cl}}[x(\cdot)]-\theta)\exp\{iS[x(\cdot)]/\hbar\}$$

and

$$\chi_V(\theta)=\int_{x_1,t_1}^{x_2,t_2} Dx(\cdot)\delta(\Theta_{ab}^{\rm cl}[x(\cdot)]-\theta) \times\exp\{iS_V[x(\cdot)]/\hbar\} .$$

Using Eq. (10.2), we have

$$\chi(\theta)=\exp(-iu\theta/\hbar)\chi_V(\theta)$$

and the transition amplitude is now given by a simple quadrature

$$g(x_2,t_2|x_1,t_1)=\int_{\theta_1}^{\theta_2}\exp(-iu\theta/\hbar)\chi_V(\theta)d\theta , \quad (10.4)$$

where θ_1 and θ_2 are the smallest and largest values that $\Theta_{ab}^{\rm cl}[x(t)]$ takes on those Feynman paths which connect (x_1,t_1) with (x_2,t_2), respectively. The effect of the perturbation in the integral (10.4) can now be analyzed in a similar way to that discussed in Sec. IX. However, *this is no longer a traversal-time analysis.* Rather we have used a different representation and in general there does not exist a simple relation between $\chi_V(\theta)$ and $\eta_V(\tau)$. Thus we conclude that a traversal-time analysis is restricted to problems for which $\Delta S[x(t)]=f(t_{ab}^{\rm cl}[x(t)])$.

XI. CONCLUDING REMARKS

In this section, we summarize our answers to two frequently asked questions about the quantum traversal (tunneling) time and also discuss the connection with a complex-valued traversal time.

A. How long does it take a quantum particle to tunnel?

First, we note that this question should be replaced by a more precise one, e.g., what is the net duration a particle spends in $[a,b]$? For a quantum particle this duration is not a single time; rather there is a distribution of times. For fixed energy scattering, this distribution is given by the traversal-time wave function $\eta(k,\tau)$, which is the probability amplitude for the duration to equal τ.

In order to obtain further information, a measurement of the traversal time must be made. This projects $\eta(k,\tau)$ onto a state localized on the τ axis. An equivalent statement is that the measuring device (e.g., a Larmor clock) excludes all Feynman paths except those for which $t_{ab}^{\rm cl}[x(t)]$ equals τ. Like dynamical variables, the traversal time obeys the usual quantum-mechanical rules.

We now examine some of the above statements in more detail.

(a) The classical traversal time $t_{ab}^{\rm cl}[x(t)]$ is only one of many time parameters that occur in classical mechanics. In a quantum treatment, it is first of all necessary to decide which classical functional is to be quantized. Time parameters other than $t_{ab}^{\rm cl}[x(t)]$ can be used, as discussed in Secs. II and X.

(b) The traversal-time wave function $\eta(k,\tau)$ is obtained by summing the Feynman weight $\exp\{iS[x(\cdot)]/\hbar\}$ over those paths which spend a duration τ in $[a,b]$. For a free particle, $\eta_0(k,\tau)$ is a complex-valued distribution (generalized function), which has an oscillatory series representation over the poles of the transmission amplitude $T_0(k,W)$. However, in applications, $\eta_0(k,\tau)$ is typically convoluted with a smooth function of finite width, as illustrated in Fig. 2.

(c) The complicated form of $\eta_0(k,\tau)$ prevents us from characterizing its properties in terms of a single time parameter, e.g., its first moment or median. Rather Sec. IV B shows that a variety of time parameters, such as the classical traversal time τ_0, the width of the semiclassical peak $\Delta\tau\approx\tau_0/[2(2\beta)^{1/2}]$, and the lifetime associated with the leading pole $\tau_{\max}=\hbar/{\rm Im}W_1$, are "hidden" in $\eta_0(k,\tau)$. A unique traversal time is only obtained in the (semi)classical limit where $\eta_0(k,\tau)\to\delta(\tau-\tau_0)$.

(d) The nonlocal nature of $t_{ab}^{\rm cl}[x(t)]$ has an important consequence for its measurement. It is well known that measurement of a local dynamical variable, such as position or momentum, causes collapse of the wave function. Because $t_{ab}^{\rm cl}[x(t)]$ is nonlocal, interaction with a measuring device (and hence disturbance of the particle's motion) must occur throughout the motion. This is clearly illustrated in our analysis of a Larmor clock measurement in Sec. VII, where the Larmor clock introduces an uncertainty ΔW into the composite potential. Note also that in Eq. (7.5), the apparatus function $G^{\rm PFS}(\phi_k^{(j)}-\omega\tau)$ only depends on the parameters of the clock, while $\eta(k,\tau)$ is the traversal-time wave function in the absence of the clock.

It is interesting to note that the original Baz' method [30] proposed to measure the traversal time without perturbing the particle's motion, which is responsible for the failure of this approach. In the Baz' method $\Delta W\to 0$, and it then follows from the uncertainty relation $\Delta\tau\Delta W\gtrsim\hbar$ that $\Delta\tau\to\infty$, i.e., there is an infinite uncertainty in the value of the traversal time.

(e) A remarkable feature of a Larmor clock measurement is that the traversal-time probability distribution depends crucially on the resolving power of the clock R_j. For example, a free particle at high energy shows Larmor clock readings peaked around τ_0 (see Fig. 6). However, for $R_j\to 0$, the results of the measurement are distributed exponentially, as discussed in Sec. VIII. In the case of resonance tunneling, Fig. 8 shows how a resonance affects the traversal-time distribution. In contrast, at higher resolution, Fig. 9 exhibits multiple reflections as the particle bounces between the potential walls.

B. How can one use the quantum traversal time?

We have described two uses of the traversal-time wave function in this paper, provided the action can be written in the form $S[x(t)]=S_0[x(t)]+\Delta S[x(t)]$, where $\Delta S[x(t)]=f(t_{ab}^{\rm cl}[x(t)])$.

(a) If the traversal-time wave function for the action $S_0[x(t)]$ is $\eta_0(k,\tau)$, then the full wave function is given by the simple result

$$\eta(k,\tau)=\exp[if(\tau)/\hbar]\eta_0(k,\tau) .$$

For example, knowing the free-particle wave function, we obtained in Sec. VI the wave function for a rectangular

barrier, a purely imaginary optical potential and for interaction with a slow oscillator.

(b) The corresonding transmission amplitude is given by

$$T(k)=\int_0^\infty \exp[if(\tau)/\hbar]\eta_0(k,\tau)d\tau \ . \tag{11.1}$$

This integral representation lets us analyze the effect of the interaction $f(t_{ab}^{\rm cl}[x(t)])$ on the unperturbed transmission amplitude. In particular, it may be possible to carry out a fast or slow analysis of the kind described in Sec. IX. Another possibility is to obtain the semiclassical limit of Eq. (11.1) by examining the stationary phase (or saddle point) structure of $\exp[if(\tau)/\hbar]\eta_0(k,\tau)$, as we have described in Ref. [15].

C. Connection with a complex-valued traversal time

A complex-valued time, obtained as a Feynman average of $t_{ab}^{\rm cl}[x(t)]$, has been introduced by Baskin and one of the present authors (D.S.) [7]; its properties are examined in Refs. [8–14]. In the traversal-time wave-function approach, this complex time is the first moment of $\eta(k,\tau)$, as has been shown in Ref. [13] for an arbitrary potential $V(x)$ and by Fertig for a rectangular barrier potential [18,19].

The complex time arises naturally [14] in an indirect measurement when one attempts to measure the traversal time without destroying the interference between Feynman paths which spend different durations in the region of interest, e.g., the Baz' method mentioned above. We have discussed the relation between this complex time and (real) observable quantities in detail in Ref. [12]. Many other tunneling times have been defined in the literature and their connection with the complex time is extensively reviewed in Refs. [1] and [4].

ACKNOWLEDGMENTS

Support of this research by the United Kingdom Science and Engineering Research Council and the Consejeria de Educacion del Gobierno Canario (Spain) is gratefully acknowledged.

[1] E. H. Hauge and J. A. Støvneng, Rev. Mod. Phys. **61**, 917 (1989); C. R. Leavens and G. C. Aers, in *Scanning Tunneling Microscopy and Related Methods,* Vol. 184 of *NATO Advanced Study Institute, Series E: Applied Sciences,* edited by R. J. Behm, N. Garcia, and H. Rohrer (Kluwer, Dordrecht, 1990), pp. 59–76; M. Büttiker, in *Electronic Properties of Multilayers and Low Dimensional Semiconductor Structures,* Vol. 231 of *NATO Advanced Study Institute, Series B: Physics,* edited by J. M. Chamberlain, L. Eaves, and J.-C. Portal (Plenum, New York, 1990), pp. 297–315; R. Landauer, Ber. Bunsenges, Phys. Chem. **95**, 404 (1991); A. P. Jauho, in *Hot Carriers in Semiconductor Nanostructures: Physics and Applications,* edited by J. Shah (Academic, Boston, 1992), pp. 121–151; M. Jonson, in *Quantum Transport in Semiconductors,* edited by D. K. Ferry and C. Jacoboni (Plenum, New York, 1992), pp. 193–238; V. S. Olkhovsky and E. Recami, Phys. Rep. **214**, 339 (1992); R. Landauer and Th. Martin, Rev. Mod. Phys. **66**, 217 (1994).

[2] A. B. Nassar, Phys. Rev. A **38**, 683 (1988); T. P. Spiller, T. D. Clark, R. J. Prance, and H. Prance, Europhys. Lett. **12**, 1 (1990); M.-Q. Chen and M. S. Wang, Phys. Lett. A **149**, 441 (1990); C.R. Leavens, Solid State Commun. **77**, 571 (1991); M. J. Hagmann, *ibid.* **86**, 305 (1993).

[3] C. R. Leavens, Solid State Commun. **74**, 923 (1990); **76**, 253 (1990); Phys. Lett. A **178**, 27 (1993); C. R. Leavens and G. C. Aers, Solid State Commun. **78**, 1015 (1991); in *Scanning Tunneling Microscopy III,* edited by R. Wiesendanger and H.-J. Güntherodt (Springer, Berlin, 1993), pp. 105–140; W. R. McKinnon and C. R. Leavens (unpublished).

[4] C. R. Leavens, Found. Phys. (to be published).

[5] R. P. Feynman, Rev. Mod. Phys. **20**, 367 (1948).

[6] R. P. Feynman and A. R. Hibbs, *Quantum Mechanics and Path Integrals* (McGraw-Hill, New York, 1965).

[7] L. M. Baskin and D. G. Sokolovskii, Izv. Vyssh. Uchebn. Zaved. Fiz. No. 3, 26 (1987) [Sov. Phys. J. **30**, 204 (1987)].

[8] D. G. Sokolovskii and L. M. Baskin, Zh. Tech. Fiz. **55**, 1838 (1985) [Sov. Phys. Tech. Phys. **30**, 1076 (1985)].

[9] D. G. Sokolovskii, Izv. Vyssh. Uchebn. Zaved. Fiz. No. 3, 52 (1988) [Sov. Phys. J. **31**, 217 (1988)]; in Ref. [1], for "261" read "621."

[10] D. Sokolovski and L. M. Baskin, Phys. Rev. A **36**, 4604 (1987); in Eq. (4.7), for "$\exp(2i\delta_2)$" read "$\exp[2i(\delta_2-\delta_1)]$"; in Ref. [1] for "261" read "621."

[11] D. Sokolovski and P. Hänggi, Europhys. Lett. **7**, 7 (1988); in Ref. [1], for "261" and "621."

[12] D. Sokolovski and J. N. L. Connor, Phys. Rev. A **42**, 6512 (1990); in Ref. [3], for "G.A." read "G.C."

[13] D. Sokolovski and J. N. L. Connor, Phys. Rev. A **44**, 1500 (1991).

[14] D. Sokolovski and J. N. L. Connor, Phys. Rev. A **47**, 4677 (1993); in Ref. [7], for "(1965)" read "(1967)" and for "305 (1987)" read "305 (1988)."

[15] D. Sokolovski and J. N. L. Connor, Solid State Commun. **89**, 475 (1994); on the line before Eq. (23), for "$(0,\infty \exp(-i\pi/4))$" read "$[0,\infty \exp(-i\pi/4))$"; in Ref. [5], for "MeV to MeV" read "meV to MeV."

[16] C. R. Leavens, Solid State Commun. **68**, 13 (1988); **68**, No. 5, ii(E) (1988).

[17] L. S. Schulman and R. W. Ziolkowski, in *Path Integrals from meV to MeV,* Third International Conference, Bangkok, 1989, edited by V. Sa-yakanit, W. Sritrakool, J.-O. Berananda, M. C. Gutzwiller, A. Inomata, S. Lundqvist, J. R. Klauder, and L. Schulman (World Scientific, Singapore, 1989), pp. 253–278. In Eq. (51), for "$a/2$" read "am."

[18] H. A. Fertig, Phys. Rev. Lett. **65**, 2321 (1990).

[19] H. A. Fertig, Phys. Rev. B **47**, 1346 (1993).

[20] P. Hänggi, in *Lectures on Path Integration, Trieste, 1991,* edited by H. A. Cerdeira, S. Lundqvist, D. Mugnai, A. Ranfagni, V. Sa-yakanit, and L. S. Schulman (World Scientific, Singapore, 1993), pp. 352–365.

[21] D. Mugnai, A. Ranfagni, R. Ruggeri, and A. Agresti, Phys. Rev. Lett. **68**, 259 (1992).

[22] W. Jaworski and D. M. Wardlaw, Phys. Rev. A **48**, 3375 (1993).

[23] A. Messiah, *Quantum Mechanics,* translated from the

French by G. M. Temmer (North-Holland, Amsterdam, 1961), Vol. 1.

[24] L. I. Schiff, *Quantum Mechanics*, 3rd ed. (McGraw-Hill, Tokyo, 1968), p. 103.

[25] G. A. Korn and T. M. Korn, *Mathematical Handbook for Scientists and Engineers, Definitions, Theorems and Formulas for Reference and Review*, 2nd ed. (McGraw-Hill, New York, 1968), p. 846, item (21.6-49).

[26] L. Schulman, Phys. Rev. **176**, 1558 (1968); L. S. Schulman, *ibid.* **188**, 1139 (1969); A. Norcliffe and I. C. Percival, J. Phys. B **1**, 774 (1968); J. S. Dowker, Ann. Phys. (N.Y.) **62**, 361 (1971); L. S. Schulman, *Techniques and Applications of Path Integration* (Wiley, New York, 1981), pp. 193–195; M. G. E. da Luz and B. K. Cheng, J. Phys. A **25**, L1043 (1992).

[27] A. Galindo and P. Pascual, *Quantum Mechanics I*, translated by J. D. García and L. Alvarez-Gaumé (Springer, Berlin, 1990), Chap. 4.6.

[28] E. Merzbacher, *Quantum Mechanics*, 2nd ed. (Wiley, New York, 1970), Chap. 6.

[29] M. R. Spiegel, *Complex Variables with an Introduction to Conformal Mapping and its Applications* (Schaum, New York, 1964), p. 175.

[30] A. I. Baz', Yad. Fiz. **4**, 252 (1966) [Sov. J. Nucl. Phys. **4**, 182 (1967)]; **5**, 229 (1967) [**5**, 161 (1967)].

[31] V. F. Rybachenko, Yad. Fiz. **5**, 895 (1967) [Sov. J. Nucl. Phys. **5**, 635 (1967)]; M. Büttiker, Phys. Rev. B **27**, 6178 (1983); C. R. Leavens and G. C. Aers, Solid State Commun. **63**, 1101 (1987), **67**, 1135 (1988); J. Vac. Sci. Technol. A **6**, 305 (1988); Phys. Rev. B **40**, 5387 (1989); J. P. Falck and E. H. Hauge, *ibid.* **38**, 3287 (1988); Z. Huang, P. H. Cutler, T. E. Feuchtwang, R. H. Good, Jr., E. Kazes, H. G. Nguyen, and S. K. Park, J. Phys. (Paris) Colloq. **49**, C6-17 (1988); W. Jaworski and D. M. Wardlaw, Phys. Rev. A **43**, 5137 (1991); Ph. A. Martin and M. Sassoli de Bianchi, J. Phys. A **25**, 3627 (1992); J. G. Muga, S. Brouard, and R. Sala, J. Phys.: Condens. Matter **4**, L579 (1992).

[32] A. Peres, Am. J. Phys. **48**, 552 (1980).

[33] C. Foden and K. W. H. Stevens, IBM J. Res. Dev. **32**, 99 (1988).